

University of Montana

ScholarWorks at University of Montana

Graduate Student Theses, Dissertations, &
Professional Papers

Graduate School

2012

USING LANDSAT IMAGERY TO EVALUATE LANDSCAPE-LEVEL IMPACTS OF NATURAL GAS FIELD DEVELOPMENT: TAZOVSKY PENNINSULA, RUSSIA, 1984-2007

Jesse Stevens Wallace
The University of Montana

Follow this and additional works at: <https://scholarworks.umt.edu/etd>

Let us know how access to this document benefits you.

Recommended Citation

Wallace, Jesse Stevens, "USING LANDSAT IMAGERY TO EVALUATE LANDSCAPE-LEVEL IMPACTS OF NATURAL GAS FIELD DEVELOPMENT: TAZOVSKY PENNINSULA, RUSSIA, 1984-2007" (2012). *Graduate Student Theses, Dissertations, & Professional Papers*. 1157.
<https://scholarworks.umt.edu/etd/1157>

This Thesis is brought to you for free and open access by the Graduate School at ScholarWorks at University of Montana. It has been accepted for inclusion in Graduate Student Theses, Dissertations, & Professional Papers by an authorized administrator of ScholarWorks at University of Montana. For more information, please contact scholarworks@mso.umt.edu.

USING LANDSAT IMAGERY TO EVALUATE LANDSCAPE-LEVEL IMPACTS OF
NATURAL GAS FIELD DEVELOPMENT:
TAZOVSKY PENNINSULA, RUSSIA, 1984-2007

By

JESSE STEVENS WALLACE

B.A. Anthropology, Northern Arizona University, Flagstaff, AZ, 2002

Thesis

presented in partial fulfillment of the requirements
for the degree of

Master of Science
in Geography

The University of Montana
Missoula, MT

June, 2012

Approved by:

Dr. Stephen Sprang, Associate Provost for Graduate Education
Graduate School

Dr. Anna E. Klene, Chair
Department of Geography

Dr. David Shively
Department of Geography

Dr. Carl Seielstad
Department of Forestry Management

Dr. Samuel Cushman
United States Forest Service

Wallace, Jesse S., M.S., May 2012
Geography

Using Landsat Imagery to Evaluate Landscape-level Impacts of Natural Gas Field Development:
Tazovsky Peninsula, Russia, 1984-2007

Chairperson: Dr. Anna E. Klene

Abstract

The Yamburg gas condensate field in northwestern Siberia sits atop the largest natural gas and petroleum basin in the world. Infrastructure related to the extraction and transport of natural gas is both geographically widespread, and has been shown to affect a much larger area than the immediate infrastructural footprint. Because field studies of the environmental impacts of development are often costly or unfeasible given the remoteness of these areas and access restrictions, the use of remote-sensing technologies is a valuable asset for assessing and quantifying disturbance over large areas.

Freely available 30 meter resolution Landsat imagery from 1984 to 2007 was employed in this thesis to quantify the effects of natural gas infrastructure on the adjacent tundra using three methods: a landscape fragmentation analysis, mean and change in mean NDVI analyses, and a cross-tabulation analysis. These analyses show that the tundra has become increasingly fragmented during the study period, and that mean NDVI values in areas adjacent to development are lower than those calculated for undisturbed areas. As distance from the infrastructural footprint increases, differences in mean NDVI decrease, approaching undisturbed values at approximately 90 – 150 m. Additionally, analysis of changes in mean NDVI values over time indicate that new infrastructure development has a depressing effect on adjacent NDVI values, while areas that have been consistently developed show a vegetation recovery response evidenced by positive changes in NDVI values when compared to undisturbed areas. Cross-tabulation of the changes in NDVI values between analysis dates indicate that these changes can be attributed to the conversion of vegetated areas to bare ground or water in the case of new development, and conversion from bare ground or water to vegetation in areas that have been consistently developed.

Acknowledgements

I would like to thank my advisor, Dr. Anna Klene, and the members of my committee: Drs. Shively, Seielstad, and Cushman for their guidance and support throughout this process.

This research would not have been possible without the opportunity to travel to the Yubileinoe, Zapalyrnoe, and Yamburg gas fields in western Siberia during the summer of 2007. I would like to thank Drs. Shiklomanov, Grebenets, Kurchatova, and Pfeiffer for sharing their experience and expertise during our time in the field. Additionally, travel funding and logistics to Russia and back were provided by the University of Montana and Moscow State University. Gazprom, NadymGasprom, and Yamburggazdobycha granted special access to their fields and provided logistical support. The Russian office of Conoco-Phillips provided additional transportation, accommodations, and meals.

Thank you to my family and friends who have patiently supported me as I meandered through this process for the better part of the last six years.

Table of Contents

Acknowledgements.....	iii
1 Introduction.....	1
1.1 Objectives.....	2
1.2 Research Questions	3
2 Background	5
2.1 Study Area.....	5
2.1.1 History of development.....	7
2.1.2 Climate and vegetation	7
2.2 Anthropogenic impacts in Arctic areas	9
2.3 Arctic land-cover classifications	12
3 Methods.....	14
3.1 Data Preparation.....	14
3.1.1 Satellite imagery	14
3.1.2 Infrastructure data layers.....	17
3.1.3 Fragmentation inputs	19
3.1.4 Control areas	20
3.1.5 Field data.....	21
3.2 Fragmentation Analysis.....	22
3.2.1 Background.....	22
3.2.2 Methods.....	24
3.3 NDVI Analysis.....	25
3.3.1 Background.....	25
3.3.2 Calculating NDVI for Landsat and MODIS imagery.....	26
3.3.3 Buffer Creation	27
3.3.4 Mean NDVI values of developed and control areas	28
3.3.5 Analyzing differences in mean NDVI values between time slices according to development status.....	30
3.3.6 Cross tabulation of mean NDVI changes.....	31
4 Results and Discussion	34
4.1 Fragmentation Analysis.....	34
4.2 Mean NDVI values of developed and control areas	36
4.3 Delta mean NDVI between time slices according to development status.....	39
4.4 Cross tabulation of change in mean NDVI	43
4.4.1 Cross tabulation of change from 1987 to 1999.....	44
4.4.2 Cross tabulation of change from 1999 to 2007.....	47
4.4.3 Discussion.....	49
5 Conclusions and Future Research.....	52
5.1 Conclusions	52
5.2 Analysis limitations and future research	53
6 References.....	57
Appendices.....	61

List of Figures

Figure 1. Study area location.	6
Figure 2. Examples of surface-water ponding adjacent to buried natural gas transportation pipelines.	9
Figure 3. An example of impacts of infrastructural development.	11
Figure 4. The SLC-off error example.	16
Figure 5. Digitized infrastructure footprint for each time slice.	18
Figure 6. An illustration of the expansion of the infrastructural footprint of the Yamburg gas field at each time slice.	18
Figure 7. An illustration of the data layers created for the fragmentation analysis.	19
Figure 8. The location of the two control areas relative to the 1987 infrastructure overlaid on the NDVI image for that year.	21
Figure 9. Examples of anthropogenic development in the study area. Above-ground pipelines near Yamburg (A), and a natural gas processing facility (B).	22
Figure 10. NDVI values for each analysis time slice.	27
Figure 11. An example of nested buffers created for developed areas.	28
Figure 12. An illustration of the extraction of control areas and development buffers from the NDVI imagery	29
Figure 13. The results of the reclassification of NDVI values for each Landsat scene.	33
Figure 14. Mean NDVI values calculated for distance intervals from the extent of infrastructural development at each time interval.	37
Figure 15. An illustration of the different extents employed in the calculation of change in mean NDVI values between two images.	39
Figure 16. Changes in mean NDVI (delta NDVI) for areas adjacent to new development.	40
Figure 17. Changes in mean NDVI (delta NDVI) for areas adjacent to existing development.	41
Figure 18. Example cross tabulation outputs.	44
Figure 19. Summary of directional change in NDVI pixel values between 1987 and 1999.	46
Figure 20. Summary of directional change in NDVI pixel values between 1999 and 2007.	49
Figure 21. A graph showing monthly NDVI composite values calculated from 500 m resolution MODIS sensor on Terra for 2000 and 2007.	51

List of Tables

Table 1. Summary of remotely sensed satellite imagery employed in the analysis.	15
Table 2. A list of fragmentation metrics calculated for the study area at each time slice.	24
Table 3. Raw NDVI value reclassification to facilitate the cross tabulation analysis.	32
Table 4. Summary of calculated fragmentation metric outputs for each image.	34
Table 5. Summary of conversion between vegetated and unvegetated classes in areas of new development between 1987 and 1999.....	45
Table 6. Summary of conversion between vegetated and unvegetated classes in areas of existing development between 1987 and 1999.....	46
Table 7. Summary of conversion between vegetated and unvegetated classes in areas of new development between 1999 and 2007.....	48
Table 8. Summary of conversion between vegetated and unvegetated classes in areas of existing development between 1999 and 2007.....	48
Table 9. Summary of cross tabulation results calculated for newly developed areas between 1987 and 1999.....	62
Table 10. Summary of cross tabulation results calculated for areas of existing development between 1987 and 1999.	63
Table 11. Summary of cross tabulation results calculated for newly developed areas between 1999 and 2007.....	64
Table 12. Summary of cross tabulation results calculated for areas of existing development between 1999 and 2007.	65

1 Introduction

Arctic regions are experiencing, and will continue to experience, the most pronounced effects of a warming climate (ACIA 2004). Additionally, these areas are home to vast deposits of natural energy resources (Gazprom Dobycha Yamburg 2007, EIA 2010). As Arctic regions become more accessible under warmer climatic regimes, it becomes increasingly important to examine the additional environmental impacts manifested by increasing anthropogenic activity. Arctic development is largely linked to resource extraction and transport – a trend which is exemplified by the Yamburg gas condensate field on the western coast of the Tazovsky peninsula in northern Siberia, Russia.

The Tazovsky peninsula lies within the West Siberian Basin, the largest petroleum and natural gas basin in the world (Ulmishek 2003). Vast gas and petroleum deposits underlie the majority of the region, stretching from just south of Novvy Urengoy, north through the Yamal, Tazovsky, and Gydansky peninsulas. The Yamburg gas condensate field on the Tazovsky peninsula is the third largest field in the world, producing 220-230 billion m³ of natural gas and gas condensate annually - one third of the Russia's total natural gas production (Gazprom Dobycha Yamburg 2008).

Evaluating the impacts of oil and gas development in western Siberia is of paramount importance, as Russia has the largest proven natural gas reserves in the world (1,600 trillion ft³), and is the leading exporter of natural gas products globally (EIA 2010). Natural gas comprises 50% of Russia's total energy consumption, and 44% of European natural gas imports come from western Siberian fields (IEA 2009). Though political and economic disputes led to a decrease in Russian natural gas production in 2009, gas field exploration and development is continuing in

western Siberia. As production from existing fields has begun to decline, previously undisturbed areas overlying known gas and oil deposits will be developed in order to meet domestic and international demand (EIA 2010). Evaluating the potential impacts to these areas is important as arctic regions are slow to recover from the effects of anthropogenic disturbance (Webber & Ives 1978). This thesis will address some of the impacts that natural gas field development and expansion manifests on previously undisturbed tundra environments.

1.1 Objectives

There are many avenues for exploring the environmental impacts of resource extraction and transportation, but this thesis will focus on two quantitative methods of assessing these impacts on the Tazovsky peninsula. The first is a basic fragmentation analysis that evaluates pre-defined metrics to measure the degree to which the landscape within the study area has been fragmented by the construction and expansion of the Yamburg gas field. For this question, just two land-cover classes were defined, developed and undeveloped. The second method identifies and quantifies radial impacts of infrastructure development on tundra adjacent to developed areas. This analysis employs the Normalized Differential Vegetation Index (NDVI) to assess differences between vegetation vitality in areas adjacent to gas field infrastructure, and nearby control areas of undeveloped tundra. These differences are further assessed as a function of distance from development, resulting in the ability to determine the point at which development no longer had a discernible effect on vegetation vitality in adjacent tundra areas. These analyses have been performed for two timeframes, 1987 to 1999 and 1999 to 2007, allowing examination of fragmentation statistics and radial vegetation impacts from the time of early field development to the time at which the author visited the study area.

The scope of this research necessitates discussion of several different fields of research. Fragmentation studies draw heavily on recent work in landscape ecology, while the geographic location of the study area requires an understanding of the unique characteristics of periglacial processes. The methodologies employed in the quantification of these impacts relied heavily on remotely sensed data and the use of geographic information systems.

1.2 Research Questions

The research methods employed in this thesis evaluated a series of related research questions:

Research Question I

What are the quantitative impacts that the development and expansion of the Yamburg gas condensate field has had on the Tazovsky peninsula? A fragmentation analysis of the study area will quantify changes in landscape composition and configuration within the extent of the development footprint, corresponding to the growth of the field from 1984 to 2007. Clearly, there will have been increased development and accompanying fragmentation, but quantification in this study allows comparisons with similar oil and gas developments at other sites, in other regions, and at other times in future work.

Research Question IIa

How much impact has infrastructure development on the Tazovsky peninsula had on the health of tundra vegetation in areas adjacent to the infrastructure footprint? Vegetation health, as measured using the Normalized Differential Vegetation Index (NDVI), will be assessed within concentric buffered distances from the infrastructure footprint in order to evaluate the effects of

development on vegetation vigor as a function of proximity to explicit development. It is hypothesized that measurable differences in NDVI will be most pronounced in areas immediately adjacent to infrastructure and decrease in magnitude with increasing distance from development.

Research Question IIb

Can the effects of infrastructure development on NDVI values be further evaluated in terms of initial disturbance related to new development and the recovery of vegetation communities in the years following development? An analysis of changes in mean NDVI values between newly developed areas and areas of existing development will evaluate the capability of NDVI analyses to identify the effects of disturbance and recovery using Landsat imagery. It is anticipated that cross-tabulation analysis of changes in pixel values over time will reveal the conversion from vegetated to unvegetated following disturbance and conversion from unvegetated to vegetated or water categories during recovery.

2 Background

2.1 Study Area

The Yamburg gas condensate field lies in the Yamalo-Nenets Autonomous District, informally known as Yamalia, or, the Yamal. The Yamal comprises the northernmost portion of the Tyumen oblast (similar to a province) and covers an area of roughly 750,320 km². The total population of the Yamal okrug (administrative district) is approximately 522,800 (Russian Census 2010), of which the majority live in urban centers. These centers are characterized by sprawling industrial development related to natural gas extraction and production – the primary economic resource of the region. The largest city in the region, Novy Urengoy (pop. 104,100 in 2010), serves as the commercial center and permanent residence of many of the oil and gas field workers throughout the northern Yamal (Gazprom Dobycha Yamburg 2007). Development related to the Yamburg gas condensate field stretches from the town of Yamburg on the western coast of the Tazovsky peninsula, northwest through the interior of the peninsula. The study area for this research includes the extent of explicit development related to the Yamburg gas condensate field, as well as two 100 km² control areas to the north and south of the gas field.

The town of Yamburg lies on the west coast of the Tazovsky peninsula (Figure 1), and is the only urban center within the study area. Construction of Yamburg began in 1982, as a base for workers and materials necessary for the infrastructural development of the gas field. Growth over the following 15 years resulted in a town capable of housing 10,000 permanent inhabitants (Seligman 1999), though the majority of Yamburg's population are impermanent shift workers with residences in larger cities throughout Russia (Gazprom Dobycha Yamburg 2007).



Figure 1. The location of the study area is shown within the Tazovsky Peninsula in the Yamalo-Nenets Autonomous District, Russian Federation. Imagery from ESRI basemap service 2011.

2.1.1 History of development

The urbanization and industrialization of the Yamal has occurred primarily within the last century. The Yamal okrug was established in 1930, and the discovery of commercially viable gas and petroleum deposits in the 1950s resulted in widespread industrial development (North 1972). Following the discovery of these resources, development in western Siberia grew rapidly, receiving 20% of the entire Soviet capital outlay in the following decade (North 1972). This rapid industrialization saw the construction of the three largest cities in the Yamal: Nadym in 1972, Novvy Urengoy in 1981, and Noyabrsk in 1982 (Vilchek & Bykova 1992). The only urban center to predate this industrial explosion is the administrative capital of Salekhard, which was founded in 1595.

2.1.2 Climate and vegetation

Underlain by continuous permafrost, the Tazovsky peninsula is primarily a peat tundra landscape, characterized by mosses, lichens, sedges, and shrub-level bushes (Forbes 1997). Appendix A provides a list of typical tundra vegetation species found on the Tazovsky peninsula. Tree growth is restricted to riverbanks, where increased active-layer depths allow more substantial root systems. Average temperatures range from -22°C to -26°C in January and 4°C to 15°C in July (Russian Climate Server, 2007).

Permafrost was recognized as a unique thermal property of landscapes as early as 1685 (French 2003), but it was not until the early 20th century that permafrost became the subject of explicit scientific examination. In 1924, a Permafrost Institute was established as part of the Siberian Branch of the Soviet Academy of Sciences (French 2003), and the bulk of the Institute's academic output centered on the work of Mikhail Sumgin, whose definition of permafrost as

“any earth material that remains below 0°C for at least two years” (1927, 20), is the accepted standard to this day.

Surface characteristics of areas underlain by permafrost are heavily influenced by the depth of the active layer. This refers to the portion of the ground which experiences a seasonal cycle of thawing and refreezing. The depth of the active layer is dependent on a number of factors, including land cover, soil type, soil moisture, and air temperature (French 2003).

The hydrological ramifications of this near-surface activity directly affect the proposed research. In areas of continuous permafrost, only the frozen ground nearest the surface thaws, and only during the summer months. This results in a short growing season and highly variable surface-water conditions. Construction in permafrost areas requires that the unique properties of the active layer be addressed to minimize the risk of subsidence. One of the methods employed to protect against subsidence is the construction of a foundation upon which roads or building are built. These pads insulate the permafrost from heat generated by constructed features, generally leading to an aggradation of the permafrost into the base of the pad which acts as an aquaclude preventing water drainage. In contrast, installation of an un-insulated pipeline carrying warm oil or gas generally leads to thawing of the permafrost around the structure and subsidence of the surface as the ice melts and runs off. Either mechanism can lead to ponding along the structure (Figure 2). While these impacts are not specifically addressed in this research, changes in surface hydrology may explain observed differences in vegetation vitality as discussed in section 4.3 of this document.



Figure 2. Examples of surface-water ponding adjacent to buried natural gas transportation pipelines.

2.2 Anthropogenic impacts in Arctic areas

While industrial development in Arctic regions has led to advances in permafrost engineering, the environmental impacts of this development have inspired a new generation of scientific literature. The construction of pipelines in Alaska and Siberia for petroleum transport required a renewed assessment of subsidence threats (Lachenbruch 1970). Kryuchkov (1976, 1993) outlined the potential collapse of arctic ecosystems as a result of increased industrialization, defining specific degradation zones around industrial centers. Vegetation response to air pollution as a result of smelting operations in Norilsk, Russia was examined by Toutoubalina and Rees (1999) who found that long-term exposure to these pollutants often resulted in complete eradication of forest stands in areas up to 15 km from the pollution source.

Vilchek and Bykova (1992) address the specific ecological threats to the region in their paper, “The Origins of Regional Ecological Problems within the Northern Tyumen Oblast, Russia.” Citing the construction of urban areas for the express purpose of petroleum and natural gas extraction, refinement, and transport, the authors describe the impacts of this development as

both exacerbating natural processes, and creating new anthropogenic threats to surrounding areas. Primary among these threats are, “thermocarst, solifluction, wind erosion, water erosion, [and] fires, which involve significantly larger areas than those primarily disturbed.” They were able to estimate the lateral extent of disturbance associated with a variety of anthropogenic activities, including oil and gas pipelines (100 m), road construction (40 m), prospecting and production infrastructure (50 – 500 m), and off-road vehicle disturbance (3 – 20 m; Vilchek and Bykova 1992).

Though development has slowed since the early 1990s (Forbes 1999), the total area of explicit infrastructural impacts within the Tazovsky peninsula were estimated to be 1.5% of the total land area by the mid-1990s (Bykova 1995). Khitun and Rebristaya (2002) identify the primary sources of disturbance in the Western Siberian Arctic as, “off-road vehicle movement, winter roads, exploratory drilling, sand excavation, pipeline and railway construction, temporary camps, settlements, and gas-condensing complexes.” In addition to these explicit disturbances, anthropogenic development has forced native reindeer herds to smaller and smaller areas, where there is a severe threat of vegetation degradation due to over-grazing (Vilchek and Bykova 1992, Vilchek 1995). Figure 3A and 3B illustrate some of the effects of infrastructural development on the Tazovsky peninsula.

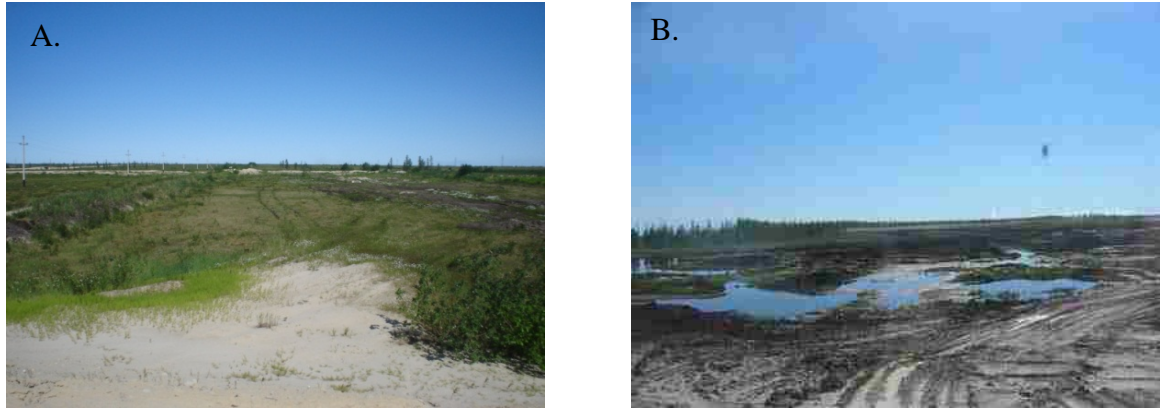


Figure 3. An example of impacts of infrastructural development. The figure on the left (A) shows the edge of a road constructed using local sand as source material. Off-road vehicle tracks and a buried pipeline are also visible. The figure on the right (B) shows the immediate impacts of disturbance related to new road construction, including excavation, ponding, and the eradication of vegetation.

The specific impacts of industrial development and resource extraction on vegetation in the Siberian Arctic have been examined extensively by Forbes (1997; 1999). Of particular interest to the current research is the finding that post-disturbance vegetation communities, while more diverse than undisturbed tundra communities, often contain species adapted to warmer and drier conditions that are not typically associated with pre-disturbance vegetation community. Non-native species often comprise 40% of post-disturbance communities (Forbes and Jeffries 1999) which can have substantial impacts on the ecosystem.

In 1987, Walker and Everett examined the impacts of road dust on adjacent tundra along the Prudhoe Bay Spine Road in northern Alaska. They found that, in addition to observable geomorphic impacts, dust generated from traffic along this road often resulted in complete eradication of adjacent vegetation within 10 m of the road, and reduced vegetative cover and less diverse species compositions within 100 m. While their study employed field-based transects to

assess localized changes in vegetation, this thesis employs remotely sensed satellite imagery to evaluate impacts over a substantially larger area.

2.3 Arctic land-cover classifications

The classification of remotely sensed imagery is integral to many raster-based GIS operations. In Russia, imagery-based mapping of vegetation macro-communities was completed as early as 1964 using aerial photography (Shchelkunova 1964). Regional descriptions and classification of tundra zones north of the polar tree line began in the 1970s (Walker et al. 1995). Recent classifications have been based on air photos at 1:25,000 scale (Kholod 1989), though satellite imagery has been employed on a limited basis (Mazhitova et al. 2004, Walker et al. 1995).

Much of the classification work in arctic regions draws upon soil data to infer vegetation types (Walker et al. 1995), or employs vegetation indices to guide the classification of vegetation types (Stow 1998; Fleming 1997). Development of high-resolution land-cover classifications, however, is typically compromised by the heterogeneous nature of tundra landscapes (Frey & Smith 2007). As a result, most classifications do not achieve a resolution that would aid in the proposed analysis. Additionally, Landsat-scale land-cover classifications of arctic regions have been shown to be highly inaccurate, with few existing data products exceeding 30-40% accuracy (Frey & Smith 2007). According to the landmark research of Anderson et al. (1976), classifications based on Landsat (and sensors with similar resolutions) are not capable of identifying land-cover types past the Level 1 classification level. In other words, the remotely-sensed imagery employed in this analysis cannot accurately identify land-cover classes into categories finer than “tundra” (Anderson et al. 1976). Other types of imagery with higher spectral or spatial resolution may allow greater differentiation of tundra vegetation but are not

available over the time period of the development evaluated in this research. This thesis will show that Landsat imagery can be used to identify landscape-level impacts that result from infrastructural development of the Tazovsky peninsula, but the research is constrained by the available imagery in its ability to identify effects on specific vegetation communities.

3 Methods

3.1 Data Preparation

3.1.1 Satellite imagery

In order to facilitate time-series analyses over a large and remote study area, satellite imagery of the Tazovsky peninsula comprises the base data for the bulk of this research. Landsat satellite imagery of the Tazovsky peninsula allowed analysis of vegetation change related to development of the Yamburg gas condensate field from 1984 through 2007. Landsat Multi-spectral Scanner (MSS) from 1984, Thematic Mapper (TM) imagery from 1987 and 1999, and Enhanced Thematic Mapper Plus (ETM+) imagery were downloaded from the University of Maryland's Global Land Cover Facility (www.landcover.org). Landsat TM imagery from 2007 was obtained through the United States Geological Survey's (USGS) Global Visualization data server (glovis.usgs.gov)¹. Though additional imagery was obtained and archived within this time period, the imagery analyzed for this research was chosen due to image integrity and lack of cloud cover. The collection dates of these images also correspond to several different stages of development of the Yamburg gas field, allowing for a chronological presentation of the growth of the field over the past 25 years. Imagery collected for use in the analysis is summarized in .

Table 1. Advanced Spaceborne Thermal Emission and Reflection Radiometer (ASTER) satellite images of the study area from June – September 2007 were obtained through the USGS's Earth Resources Observation and Science (EROS) image collection, but were unusable

¹ The analyses described in this thesis were performed prior to the availability of the full Landsat imagery archives in 2009.

for analysis purposes due to high cloud cover which compromised the ability to perform NDVI calculations.

Table 1. Summary of remotely sensed satellite imagery employed in the analysis.

Imagery	Collection date	Native pixel resolution	Resampled pixel resolution
Landsat MSS	7/24/1984	57 x 57 m	N/A
Landsat TM	7/4/1987	28.5 x 28.5 m	30 x 30 m
	09/15/1999	28.5 x 28.5 m	30 x 30 m
	7/18/2007	30 m x 30 m	30 m x 30 m
Landsat ETM+	7/10/2007	30 m x 30 m	30 m x 30 m

All satellite imagery was imported into the Idrisi® GIS software as *.tif* files.

Downloaded scenes that had different spatial projections were reprojected to the WGS 1984, UTM 44 North projection. All imagery was resampled to ensure that the individual pixels within each scene were of identical size (30 m × 30 m) and coincident extent².

During initial imagery analysis, a 2007 Landsat ETM+ scene was used. All Landsat ETM+ imagery collected after May 31, 2003 was affected by the failure of the Scan Line Corrector (SLC), which, “compensates for the forward motion of the [Landsat 7] sensor” (USGS 2009). This error manifests itself as diagonal lines of missing pixels within the Landsat scene. While the majority of each scene (approximately 80%) is unaffected by this error, affected areas are unusable for analysis purposes. In order to exclude pixels that were compromised within the 2007 imagery, a spatial mask was created corresponding to the extents of the corrupted areas within the scene. Analyses performed using 2007 imagery were based only valid pixels lying outside of the spatial mask extent (Figure 4).

² The 1984 imagery was not included in the resampling procedure due to its coarse resolution. 1984 is roughly the time of initial field construction, and no development features are detectable on the image. As such, the image serves as a baseline reference for the pristine tundra in the pre-development era.

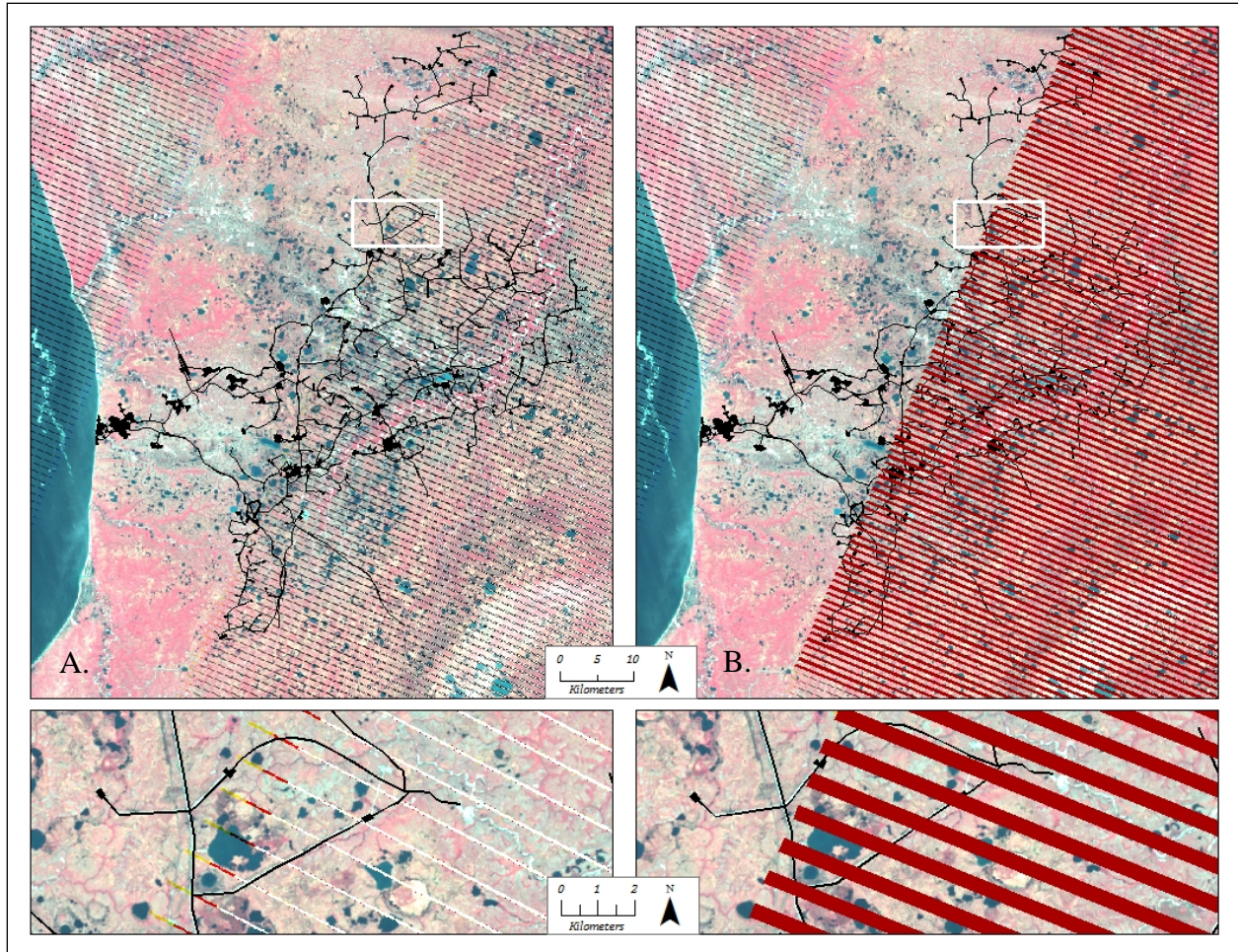


Figure 4. The SLC-off error causes linear bands of pixel errors approximately 400 m wide. This figure shows the presence of the error on false-color Landsat 7 imagery (A), and the mask created to exclude affected errors (in red) from subsequent analysis (B). The two bottom figures are enlarged from the larger scenes. Development is shown in black for reference.

While the majority of analyses described in this study were originally completed with this ETM+ imagery, error-free TM imagery became available later in the research process.

Preliminary analyses of the newly-available imagery indicated that the research would benefit from incorporation of error-free imagery. The research described in this document is based on the use of the error-free 2007 TM imagery.

3.1.2 *Infrastructure data layers*

A variety of band combinations were evaluated with regard to their ability to facilitate a spectral identification of the infrastructure footprint at each time slice. Supervised and unsupervised classification tools were attempted within the Idrisi GIS software, but were unable to reliably distinguish between developed areas and areas of exposed sand that comprises much of the alluvial and coastal features within the study area. The sand and gravel used for construction appeared to be sourced locally, so the spectral properties of the roads and beaches were identical. Feature Analyst® software was also evaluated as a potential tool for spectrally identifying developed pixels, but outputs were similarly compromised in their ability to reliably exclude undeveloped bare ground within each scene.

While spectral analysis was not sufficient to classify all infrastructure pixels independently, a spatial data layer representing the infrastructural footprint was digitized in ArcGIS 9.3 through a combination of visual interpretation, GPS data, photos, and other field-based information. During the digitization process, areas of significant development (urban areas, processing facilities, extraction pads) were drawn as polygons, while linear features (roads, pipelines) were drawn as line features. This process was repeated for each time interval, resulting in layers that represent the extent of existing infrastructure for each (Figures 5 & 6). During the digitizing process, areas that were not able to be confidently identified as an infrastructural feature were not included. This likely resulted in errors of omission during creation of the infrastructural layers, meaning that total infrastructure at each time slice is somewhat underestimated. In addition, buried and elevated pipelines were not able to be discerned with enough certainty to be included in the analysis, which clearly means that the results underestimate the true extent of fragmentation.

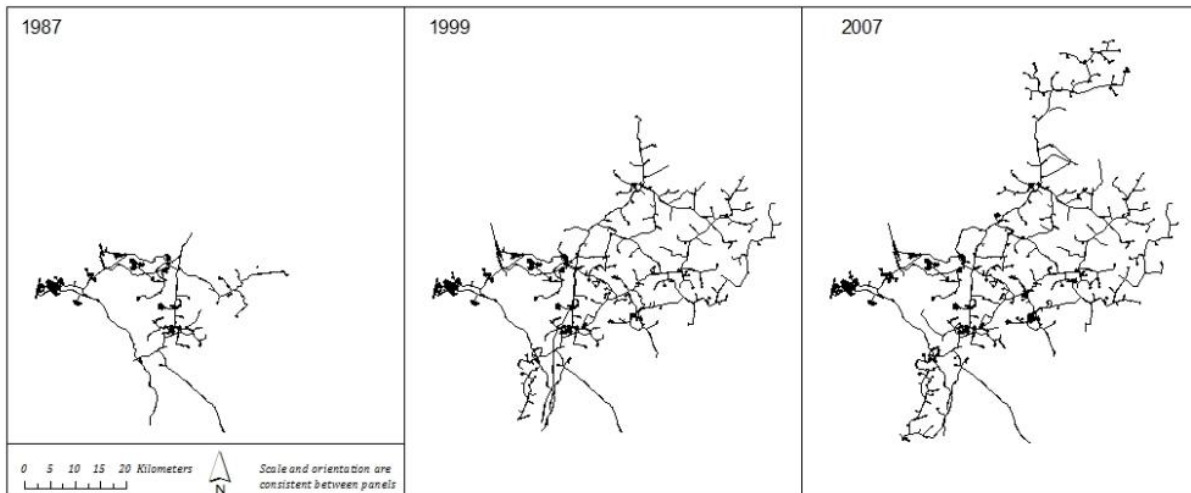


Figure 5. Digitized infrastructure footprint for each time slice.

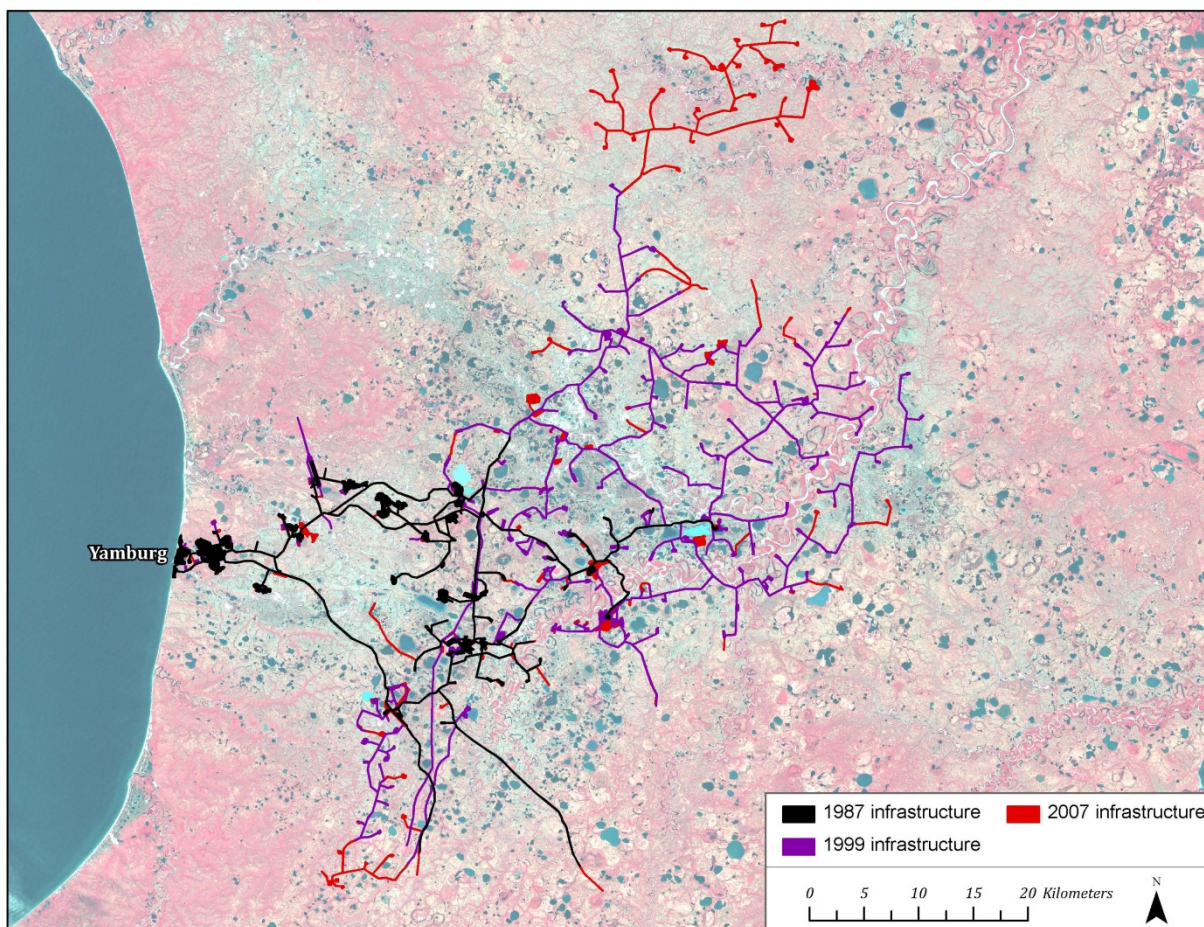


Figure 6. An illustration of the expansion of the infrastructural footprint of the Yamburg gas field at each time slice.

3.1.3 Fragmentation inputs

The software used to execute the fragmentation analysis requires the base input data to be in a raster, or raster-derived format. The digitized vector infrastructure line features were buffered by 15 m to ensure that they encompassed at least one pixel width. These buffered features were then combined with the polygons depicting development features and converted to raster files representing the areal extent of development at each time slice. These areas were then combined with another raster that encompassed all tundra areas within the largest research analysis extent, defined by a 600 m buffer from the 2007 development footprint. The raster files were classified such that the infrastructure was labeled “developed” while all background pixels (in this case, tundra with no development) were classified as “undeveloped” (Figure 7). To eliminate the possibility of false breaks or corner to corner connections between adjacent pixels during fragmentation calculation, the final raster inputs were resampled to 10 m resolution.

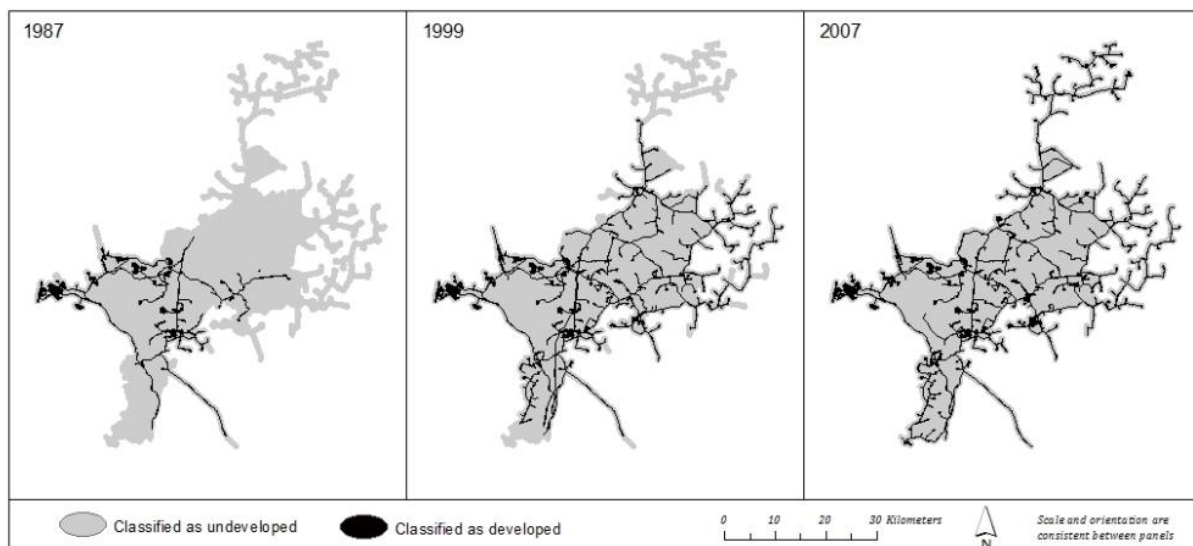


Figure 7. An illustration of the data layers created for the fragmentation analysis.

3.1.4 *Control areas*

To separate the effects of development from natural variability between time slices (climatic changes, differences in seasonality between image collection dates, variations in sensor configurations), control areas were defined for the NDVI analysis. The control areas are two 100 km² squares that lie outside of the development footprint in undisturbed tundra. These areas were chosen based upon similar geomorphic and vegetative characteristics relative to the area in which development has taken place (Figure 8). Two control areas were chosen to capture the high variability and range of NDVI values in the area. Mean values for each control area, as well as an average of both are used as the benchmarks against which to evaluate NDVI values from areas adjacent to development.

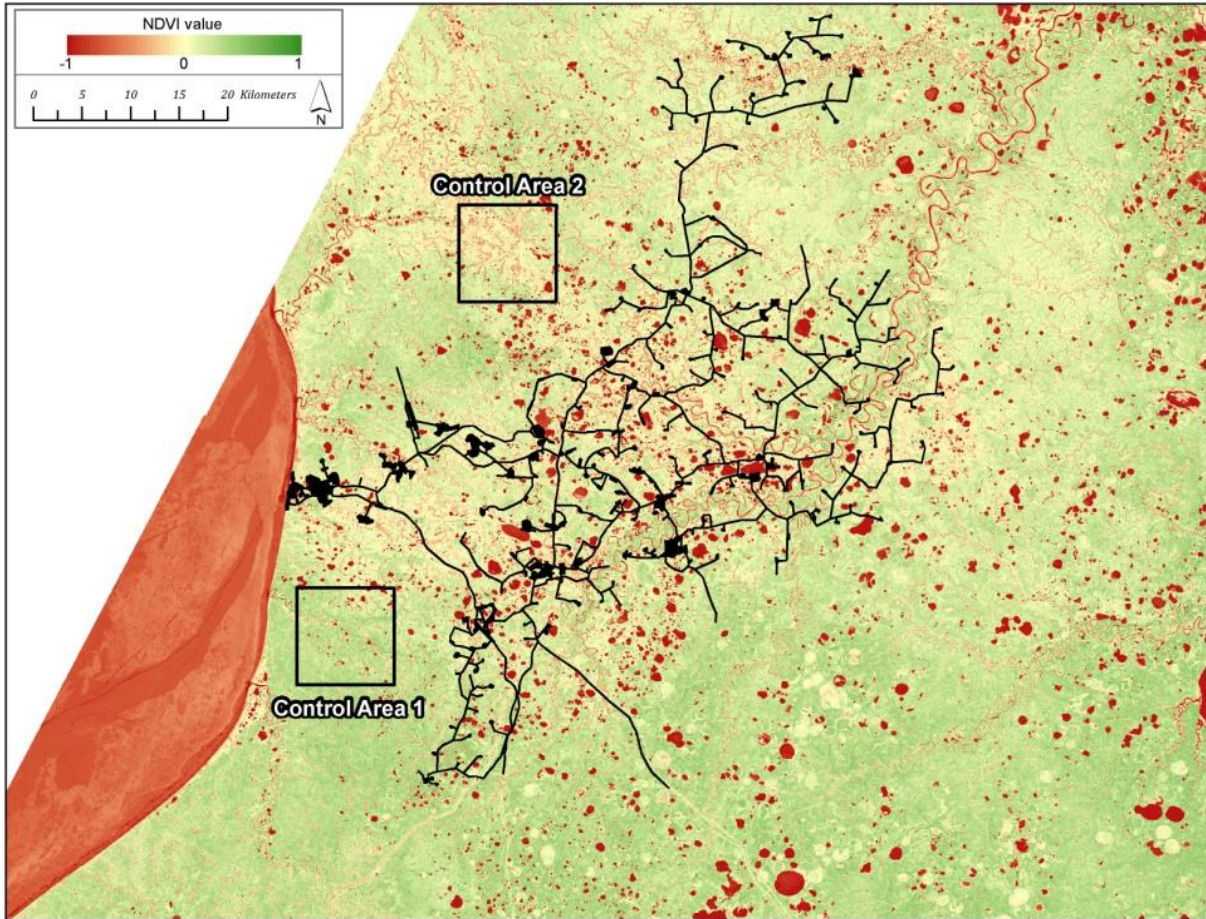


Figure 8. The location of the two control areas relative to the 2007 infrastructure overlaid on the NDVI image for that year.

3.1.5 Field data

During the summer of 2007, the author visited the Yamburg gas condensate field as part of the International Polar Year's Technogenic and Environmental Permafrost Observatories field program. Because the gas field is privately owned, areas of access and available data collection opportunities were limited.

Data collected during the field visit included photographs, GPS point data of representative land-cover features, and field maps indicating topographic features and areas of development.

Photographs and personal observations of processes relating to infrastructure development and its impacts on adjacent tundra have guided the hypotheses and analyses described in this proposal. Field maps have been used in conjunction with freely-available imagery and spatial data layers to guide the digitization of the development footprint. Figure 9 provides examples of typical industrial infrastructure in the study area.

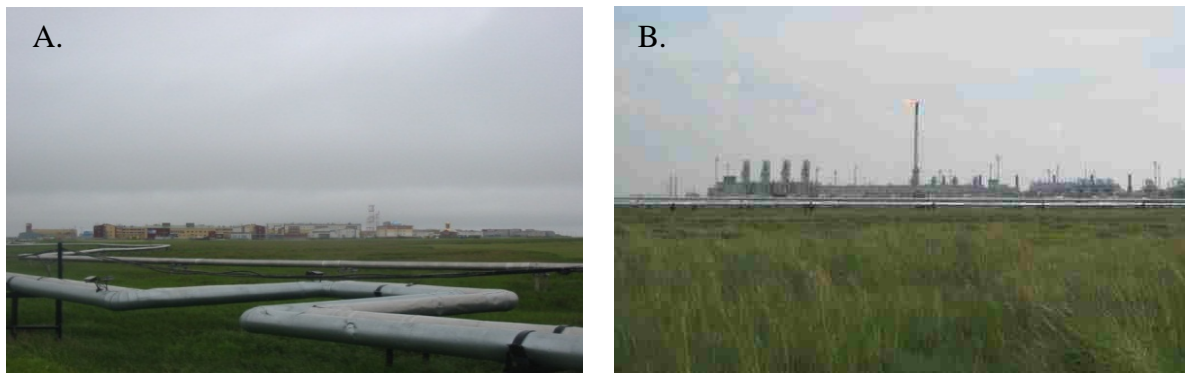


Figure 9. Examples of anthropogenic development in the study area. Above-ground pipelines near Yamburg (A), and a natural gas processing facility (B).

3.2 Fragmentation Analysis

3.2.1 Background

Within the field of landscape ecology, there is a differentiation between landscape patterning and landscape fragmentation. Landscape patterns fall under the larger umbrella of landscape structure (O'Neill et al. 1988), referring to the, “spatial relationship among distinctive ecosystems or landscape elements” (Li et al. 2001). While fragmentation studies often identify the nature of these spatial relationships, the emphasis is typically on how anthropogenic factors influence these interactions. This research does not seek to specifically address ecological impacts of Siberian industrialization, but fragmentation metrics and changes in vegetation health serve as quantitative indicators of the spatial extent and intensity of the development.

Fragmentation studies often occur within the field of wildlife biology and forestry, as habitats are analyzed with regard to logging or anthropogenic impacts (Schneider 2001; Andren 1994; Fahrig 1997; Harrison & Bruna 1999). Weller et al. (2002) address fragmentation specific to resource development in their examination of the scope of oil and gas infrastructure in Wyoming. This thesis research is based on a similar analytical design to that employed by Weller et al., in that it uses fragmentation metrics as a quantitative tool to measure the discrete impacts of resource development. Primary among their findings is that infrastructure related to the development of the natural gas field comprised nearly four percent of the total study area. Although the study area evaluated in this thesis is significantly larger, metrics calculated for the Tazovsky peninsula will provide similar data (i.e., percentage of the landscape disturbed) that allows for the comparison of the impacts of these two fields. Southworth et al. (2002) examined the use of fragmentation metrics in analyzing land-cover change through satellite imagery and found patch size to be a good indicator of economic activity. While their research included some metrics that rely on a more comprehensive land-cover classification than that employed in this research, they calculate number of patches (NP), largest patch index (LPI), and class area (CA) as basic quantitative indicators of the extent to which their study area has been fragmented. This research will calculate the same three metrics, with the inclusion of a metric that calculates the percentage of land occupied by each class (PLAND). Section 3.2.2 provides additional details on the fragmentation analysis performed for this research.

While fragmentation analyses can be performed on any classified image, additional avenues for interpretation and analysis increase as the number of discrete land-cover classes identified increase. Because the resolution of the imagery does not allow accurate land cover classifications past the 'tundra' level (Anderson et al. 1976), fragmentation metrics were

calculated based on a Boolean classification that identifies simply “disturbed” and “undisturbed” land-cover classes.

3.2.2 *Methods*

Landscape fragmentation of the study area was calculated using the statistical package FRAGSTATS[®] 3.3. This program analyzes the patterning of landscapes as defined by classified spatial data layers (McGarigal et al. 2002). Fragmentation information is conveyed through a set of metric outputs based on parameters identified by the user for each analysis. This research employs patch and class metrics to provide a quantitative summary of the extent of explicit development and the impact that development has had on the landscape structure of the study area. Patch metrics form the foundation of the fragmentation analysis for this research as the creation of isolated tundra patches by expanding infrastructure in the study area is explicitly the process that this analysis is seeking to quantify. Class metrics provide outputs on the relative extent of development in the context of the entire study area which is useful for comparisons with other fragmentation studies performed on areas of differing sizes. Because diversity indices are not informative at the Boolean classification level, they have been excluded from this analysis. The metrics calculated for this research, and a brief description of each are given in Table 2.

Table 2. A list of fragmentation metrics calculated for the study area at each time slice.

Metric	Description
Class Area (CA)	The total area occupied by each class
Patch Count (NP)	The total number of individual patches by class
Largest patch (LPI)	The area of the largest patch in the analysis area
Landscape percentage (PLAND)	Percentage of analysis area occupied by given patch type

The fragmentation analysis was performed on the digitized development layers created for each time interval described in section 3.1.3. The outputs of these metric calculations and a discussion of their meanings are provided in section 4.1.

3.3 NDVI Analysis

3.3.1 Background

The Normalized Differential Vegetation Index is a ratio of spectral band reflectance that can be performed on remotely sensed imagery that contains a red (R) and near-infrared (NIR) band. This ratio is expressed by the equation:

$$\text{NDVI} = (\text{NIR} - \text{R}) / (\text{NIR} + \text{R}).$$

Results of this equation range from -1 to +1, where values from -1 to 0.1 indicate unvegetated surfaces, including water, artificial surfaces (such as infrastructure), bare soil, ice, or cloud cover, and values above 0.1 represent increasing vegetation greenness (interpreted as vegetation vitality) as the values approach positive one (NASA 2011).

NDVI is a widely used tool for remote-sensing based vegetation analyses in arctic regions, as it captures the dynamic response of tundra vegetation to the shortened growing seasons found in high-latitude areas (Raynolds et al. 2008). Recent studies employing NDVI focus on the response of tundra vegetation to warming trends observed in arctic areas (Zhou et al. 2003; Goetz et al. 2005), as well as bioclimatic vegetation zone mapping of arctic regions (Raynolds et al. 2006).

Advanced Very High Resolution Radiometer (AVHRR) satellite imagery is widely used to monitor global NDVI responses over time at a resolution of one kilometer (USGS 2010,

Lillesand et al. 2004). AVHRR data are typically processed to present an average of NDVI values collected over a period of time. This approach minimizes variables associated with collection at a single date (cloud cover, time of day, sensor error), but the coarse resolution of this imagery is unsuitable for capturing localized differences in NDVI values at the scale necessary for this research. The Landsat imagery employed in this analysis is limited to single-scene collection dates, but provides a much finer spatial resolution that facilitates observations on changes in NDVI values at 30 m intervals.

3.3.2 *Calculating NDVI for Landsat and MODIS imagery*

The Normalized Differential Vegetation Index was calculated for each of the Landsat satellite images described in section 3.1.1. Each *.tif* raster image was imported into the Idrisi GIS software, and the NDVI value was calculated (Figure 10). Differences in the range of NDVI values are clearly visible between the June 1987, September 1999, and July 2007 images, making it difficult to interpret direct subtraction of pixel values from one year and another, and so control areas were utilized to provide context for these comparisons.

Monthly composite NDVI imagery calculated from MODIS Terra sensor was also downloaded from the USGS Land Processes Distributed Active Archive Center (LP DAAC). These data consist of mean maximum NDVI composite values calculated for 30-day periods and were used in this analysis to illustrate monthly differences in NDVI values due to seasonality. Unfortunately, MODIS data are only available from 2000 onwards and so were not available to be compared to earlier time slices. The effects of these seasonal variations revealed in the Landsat imagery described above are further discussed in Chapter 4.

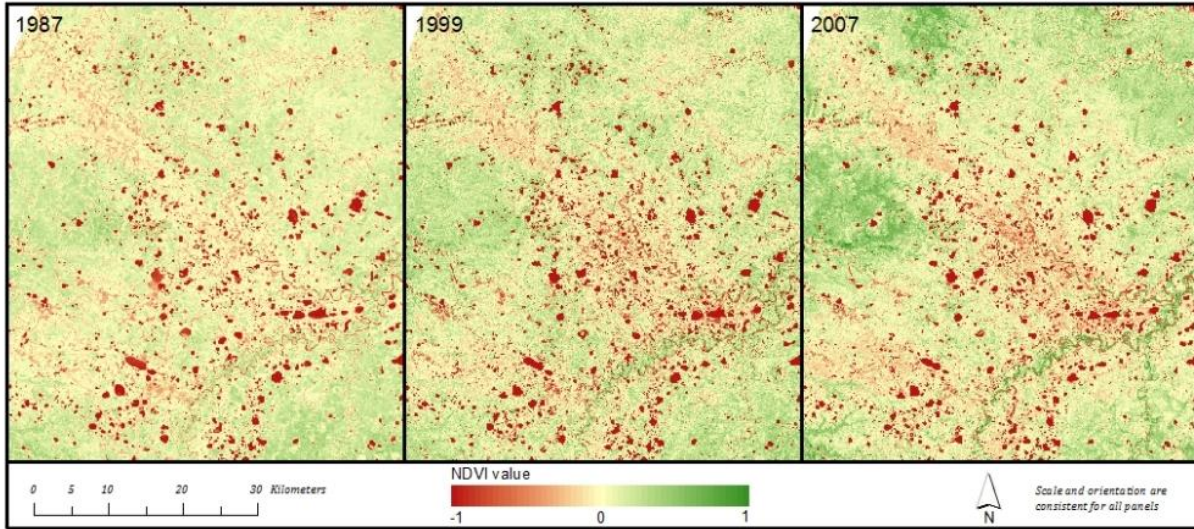


Figure 10. NDVI values for a representative area in the northwest quadrant of the study area, illustrating variability between time slices.

3.3.3 Buffer Creation

To evaluate the radial distance of impacts associated with development, a series of nested buffers surrounding the infrastructure footprint were created. The width of these buffers were equal to one pixel-width out to a distance of 150 m (i.e., 30 m, 60 m, 90 m, 120 m, 150 m) to capture the finest resolution possible given the constraints of the data. Two coarser buffers (150 – 300 m, 300 – 600 m) were also created to capture more distant impacts (Figure 11). These buffers were used to evaluate both mean NDVI values for each time slice, as well as changes in mean NDVI values over time.

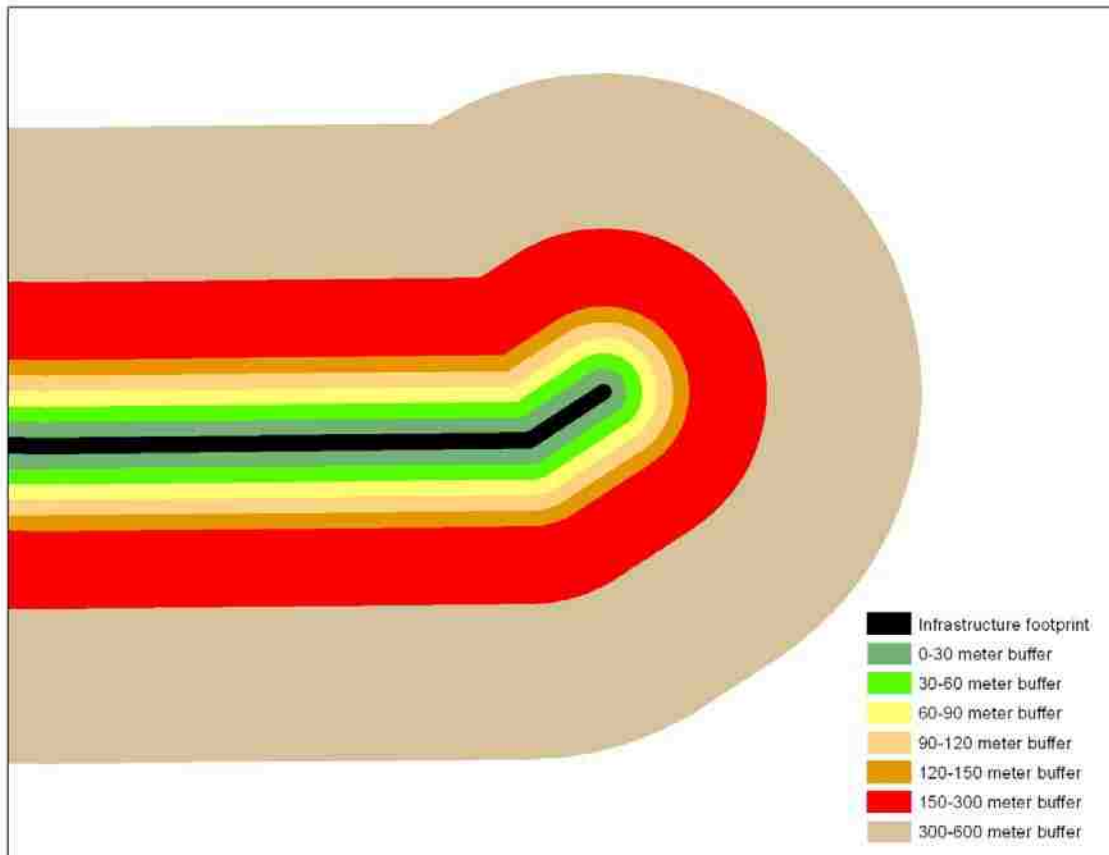


Figure 11. An example of nested buffers created for developed areas.

3.3.4 Mean NDVI values of developed and control areas

In order to evaluate NDVI differences between areas adjacent to development and undeveloped control areas, mean values were calculated for each control area, and each buffered distance interval as described in the previous section. In order to calculate these mean values, each control area and each individual buffer area was used as spatial mask to extract the specific areas of interest from the raw NDVI raster images. This extraction was performed in ArcGIS® 9.3, using the Spatial Analyst extension. Figure 12 provides an example of a buffer area and control area that have been extracted from a raw NDVI layer.

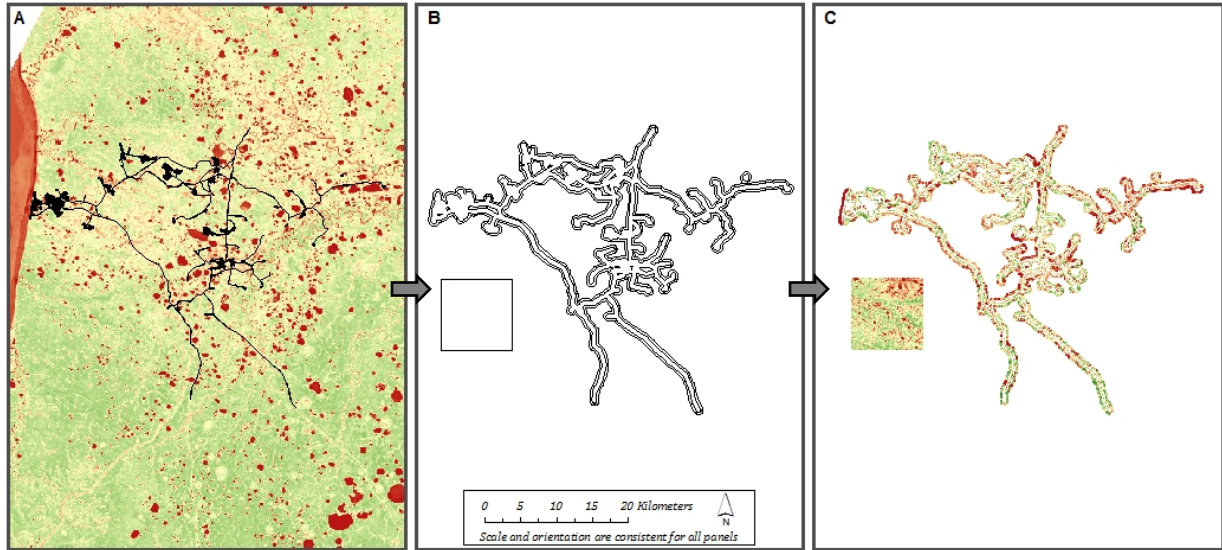


Figure 12. An illustration of the extraction of control areas and development buffers from the NDVI imagery. (A) shows the 1987 infrastructure footprint on an image of NDVI values. (B) shows the extents of the control area and the 0 – 600 m buffer. (C) shows the results of the extraction, with NDVI values for just the control area and within the extracted buffer.

NDVI values are susceptible to variation that is not explicitly the result of environmental inputs (Zhou et al. 2001). Therefore, this research does not interpret raw NDVI values as stand-alone indicators of vegetation response to development in the study area. Instead, mean NDVI values for each buffered distance interval are compared to mean NDVI values calculated for undeveloped control areas as a way of identifying relative differences between developed and undeveloped tundra vegetation. By examining these data within each buffered distance interval, it also becomes possible to determine the interval beyond which development no longer has a discernible impact on NDVI values. This manifests as the distance at which mean change values between times slices are similar in both developed and control areas.

3.3.5 *Analyzing differences in mean NDVI values between time slices according to development status*

In addition to the complications inherent in interpreting raw NDVI values calculated for tundra landscapes, the avenues for meaningful interpretation are limited temporally. To evaluate changes in NDVI over time, the mean NDVI values calculated for each time slice were evaluated with regard to the amount of change observed between time slices. This calculation (delta NDVI) allows one to determine whether or not areas adjacent to development experience greater changes in NDVI values than the changes observed within the control areas. Additionally, the direction of changes (positive indicate conversion to more vigorous vegetation, and negative indicate loss of vegetative cover) provides avenues for interpreting the localized effects of infrastructure development on the adjacent tundra.

Calculating changes in mean NDVI values over time requires a mathematical operation wherein the earlier of the two images being compared is subtracted from the later image. This operation is performed on a pixel-by-pixel basis throughout the entire image, with the pixel values forming the numeric inputs for the calculation. This calculation results in a new raster image with pixel values that represent the amount of change in NDVI values between the two time slices. Positive values indicate increased vegetative cover and/or vigor, and negative values indicate decreased vigor or conversion to a non-vegetated condition. Because NDVI values can be negative numbers for pixels representing water, subtracting raw NDVI values can result in false positive outputs if two pixels with negative values are subtracted from one another. To remedy this, negative values for each raw NDVI image were reclassified to equal zero before the subtraction. The loss of data resolution that results from this reclassification (i.e. variance in negative values) is unimportant in the context of this aspect of the research, as the analysis seeks

only to evaluate changes in vegetation health as a function of proximity to development. Change in an NDVI value from a positive number to zero between time slices conveys the same information as change from a positive number to a negative number – in both instances the pixel in question has become devegetated. Similarly, change from zero to a positive number indicates that a pixel has become vegetated where it was previously unvegetated. These reclassified NDVI data are only used to evaluate differences in change between time slices for control areas and areas adjacent to development. The specific nature of this change – which pixels are contributing to observed differences and how those differences can be interpreted are addressed with cross tabulation analysis described below.

3.3.6 Cross tabulation of mean NDVI changes

The calculation of change in mean NDVI values was performed to identify differences in vegetation response over time between areas adjacent to development and undisturbed control areas. The results of the calculations discussed above do not allow concrete observations on how the condition of the pixel changed. To identify these more fundamentally over time, a cross tabulation was performed between each control area and each development buffer at each time step. Cross tabulation is a GIS operation that identifies the specific change that each pixel in a data layer has experienced between time slices, relative to a control. This level of detail is complimentary to the delta mean NDVI analysis described in the previous section as it allows the user to identify the changes in the state of each pixel that constitute the overall differences in mean NDVI observed through time.

As discussed in the previous section, raw NDVI values are the result of a ratio calculation wherein the outputs can be any number between -1 and 1. NDVI values can be grouped into ranges that have inherent meaning, which allows a meaningful discussion on the nature of the

observed changes. Weier and Herring (2011) suggest that NDVI values ranging from -1 to 0.1 represent unvegetated surfaces, values from 0.1 to 0.3 represent shrub and grasslands, and values above 0.6 represent lush temperate and tropical forests. These values, and examination of NDVI values calculated for the Landsat scenes employed in this imagery, were used to create a reclassification matrix that defines meaningful class definitions for the cross-tabulation analysis (Table 3). Figure 13 shows the results of the reclassification performed to support the cross-tabulation analysis.

Table 3. A description of the reclassification performed on the raw NDVI values to facilitate the cross tabulation analysis.

Raw NDVI values	New class	Class interpretation
-1 to -0.2	1	Deep water, shadows
-0.2 to 0.1	2	Bare ground, snow cover, clouds, shallow water
0.1 to 0.3	3	Sparse or light green vegetation
0.3 to 0.5	4	Intermediate vegetation
0.5 to 1	5	Vigorous green vegetation

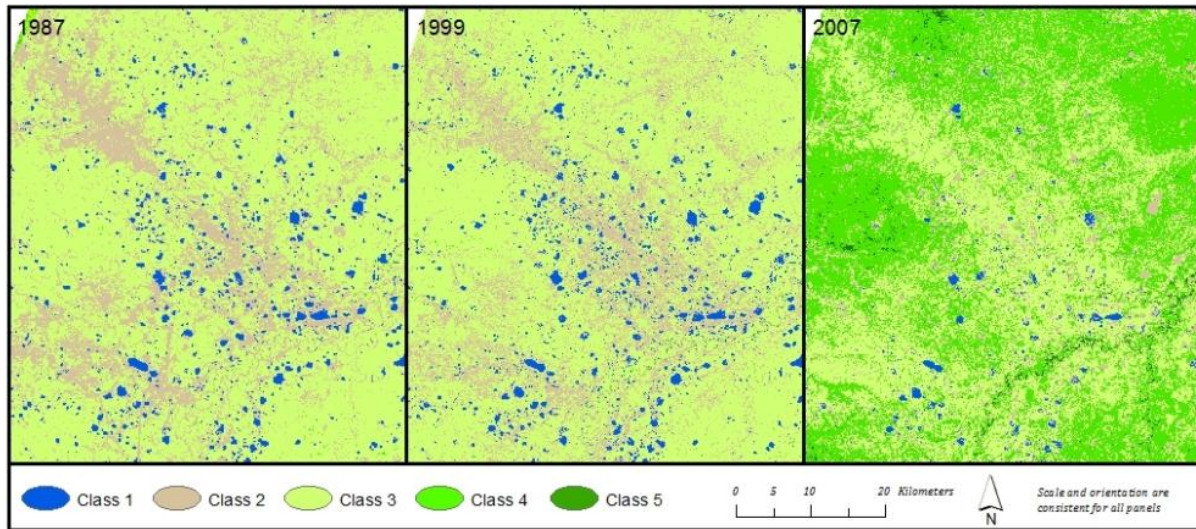


Figure 13. The results of the reclassification of NDVI values for a representative area in the northwest quadrant of the study area for each Landsat scene. 2007 NDVI values are somewhat higher than the earlier scenes, because of phenological differences. Categorizing the data using one scale resulted in over-stating the vigor of the vegetation.

The cross tabulation operation was performed using the *Crosstab* tool in the Idrisi GIS software. Cross tabulation results are discussed in section 4.4.

While differences in seasonality were apparent in the reclassified 2007 image, other imagery with dates closer to the 1987 and 1999 images was not available. Several attempts of atmospheric correction were tried on the 2007 TM image, including dark object correction, but the results were unsatisfactory, and the analysis proceeded with the available imagery. As mentioned in section 3.1.1, this imagery was obtained and analyzed before the Landsat archive opened and so were not processed to more recent standards (Chander et al., 2009) as those were evolving during the time of this research. These issues will be discussed in greater detail in Chapter 5 of this document.

4 Results and Discussion

4.1 Fragmentation Analysis

The fragmentation analysis was conducted on a study area defined by the lateral extent of the largest disturbance buffer described in section 3.3.3. By using this largest extent (1,487.2 km²), the fragmentation metrics calculated for each time interval can be compared through time within a static area. Table 4 provides a summary of the metric outputs resulting from the fragmentation analysis performed using FRAGSTATS 3.3.

Table 4. Summary of calculated fragmentation metric outputs for each image.

Fragmentation Metric	1984	1987	1999	2007
Class Area (CA) Total (km²)	1487.2	1487.2	1487.2	1487.2
Developed	0	28.4	54.9	71.4
Undeveloped	1487.2	1458.8	1432.3	1415.8
Patch Count (NP) Total	1	30	77	86
Developed	0	7	5	17
Undeveloped	1	23	72	69
Largest patch (LPI) Total (%)	100.00	81.35	33.40	39.88
Developed	0	1.89	3.67	4.73
Undeveloped	100.00	81.35	33.4	39.88
Landscape percentage (PLAND) Total	100.00	100.00	100.00	100.00
Developed	0	1.91	3.69	4.8
Undeveloped	100.00	98.09	96.31	95.2

Metric outputs confirm intuitive assumptions concerning the impacts of industrial development on a previously undisturbed landscape. As discussed earlier, no development was visible on the 1984 imagery, which corresponds to the founding of the field in 1983 but some months being needed to construct facilities to house the workers and infrastructure required to

begin full-scale development of the field. The earliest activity focused on the port area and a sub-surface tunnel which housed material out of the weather and would be difficult to detect on Landsat imagery.

Class Area (CA) measures the total area of developed and undeveloped land at each time interval, and quantifies the expansion of infrastructural development from an undisturbed state in 1984 to 71.4 km² in 2007. The percentage of the analysis area occupied by each class (PLAND) corresponds directly with the CA metric, showing an increase in the percentage of developed land from 0% in 1984 to 4.73% in 2007. As the amount of developed land increases over time, the landscape becomes increasingly fragmented as evidenced by the number of discrete patches (NP). Patches are defined as areas of one class become disconnected from other areas of the same class. This metric is important as it illustrates how undeveloped areas have become increasingly disconnected from other undeveloped areas as the gas field has expanded. The slight decrease in the number of developed patches between 1987 and 1999 are a product of previously disconnected areas of development becoming incorporated into the larger infrastructural footprint.

The Largest Patch Index (LPI) is an additional way of illustrating increased lack of connectivity between undeveloped areas. Prior to the construction of the gas field, the entire study area comprised a single patch of undisturbed tundra, and the corresponding LPI was 100%. As infrastructural development expanded across the Tazovsky peninsula, the number of undeveloped patches increased to 69 patches in 2007, with the largest undisturbed patch now constituting only 39.9% of the study area. This represents a slight increase from the 1999 results, as some infrastructural elements appear to have been abandoned and reclaimed by vegetation during the time in between the analysis imagery dates.

The fragmentation analysis results provided here provide a basic quantitative summary of the landscape-level impacts that natural gas infrastructure development has had on the tundra of the Tazovsky peninsula. As a measure of the overall extent of development in the Yamburg gas field, the PLAND value of 4.73% is similar to the results of Weller et al. (2002) who calculated a PLAND value of 4% for the Big Piney – LaBarge oil and gas field in southwestern Wyoming. While this number is substantially larger than 1.5% total disturbance area calculated for the entire Tazovsky peninsula by Khitun and Rebristraya (2002), the analysis area used in this study was artificially constrained and did not include large tracts of undisturbed tundra to the north of the study area; Weller et al. (2002) used a similar method to define the boundary of their study area.

While this research does not explicitly address the ecological impacts of landscape fragmentation with regards to habitat connectivity, predator-prey interactions, or other biological impacts, these avenues of analysis could provide a better understanding of the comprehensive impacts of infrastructure development on the Tazovsky peninsula if higher resolution imagery were available over this time frame or more rigorous fieldwork was possible. However, given the lack of access to these protected national strategic reserves, the current method was the best possible at this time.

4.2 Mean NDVI values of developed and control areas

Mean NDVI values were calculated for both control areas and for a series of distance intervals from the infrastructure footprint at each time slice (1987, 1999, 2007). Mean NDVI values within each buffered distance interval were compared to mean NDVI values calculated

for each of the two control areas (Figure 14).

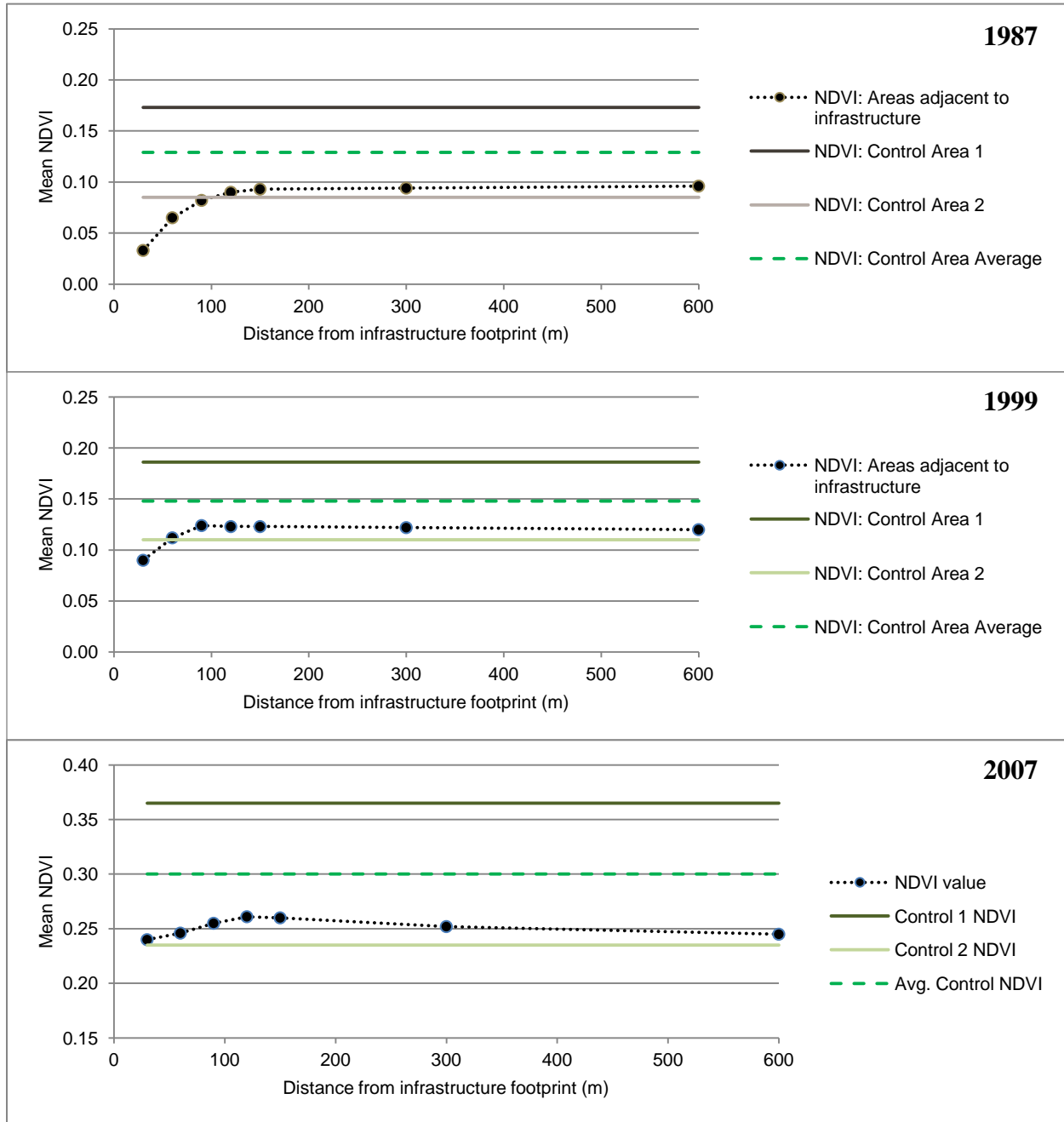


Figure 14. Mean NDVI values calculated for distance intervals from the extent of infrastructural development at each time interval. Mean NDVI values for each control area are shown for comparison.

Mean NDVI values are lower in areas immediately adjacent to the infrastructure footprint than those observed in control areas in each time slice. This difference diminishes as the distance from development increases, approaching (and in some cases exceeding) mean values calculated for control areas. Through all time slices, the distance at which NDVI values for areas adjacent to infrastructure approach what can be assumed to be the un-impacted mean for that area is between 60 m and 150 m. Due to the high variability of NDVI values in tundra landscapes, merely noting a difference in mean NDVI between control areas and areas adjacent to development has little meaning. That the mean NDVI values within the development buffers increase as distance from development increases in each time slice indicates that the presence of infrastructure has a consistent depressing effect on vegetation within 60 m of developed areas. These observations are consistent with Forbes' findings (1997, 1999) that post-disturbance vegetation is often primarily comprised of drier, non-native species as compared to undisturbed tundra communities. Observed lower NDVI values within 60 m of the infrastructure footprint are also consistent with Walker et al.'s findings (1987) that road construction in Arctic areas has observable negative effects on adjacent vegetation within 100 m of the constructed feature.

While the differences between mean NDVI in developed and control areas has meaning within one image, it is problematic to interpret differences in values between time slices using raw NDVI data. Variables that impact NDVI calculations within a given scene include temperature, precipitation, time of year, and the atmospheric conditions surrounding the data acquisition sensor at the time of collection (Zhou et al. 2001). Because these variables have not been controlled for in this research, interpretations of NDVI change over time will be addressed through an evaluation of changes in mean NDVI values between control areas and areas adjacent to development. The results of this analysis are discussed in the following section.

4.3 Delta mean NDVI between time slices according to development status

A comparison of changes in NDVI values between images was conducted to evaluate the hypothesis that areas adjacent to development will change at greater rate than undisturbed control areas as vegetation experiences initial disturbance and then recovers in response to infrastructure development. This analysis was performed upon each development buffer both for areas developed during the period defined by each time slice, as well as on areas that were previously developed. This distinction facilitates observations on the impacts of initial disturbance and the subsequent recovery of plant vegetation adjacent to developed areas. Though the time intervals between scenes employed in this analysis are significant, and are therefore unable to capture finer-resolution temporal changes, there is value in assessing the cumulative response of vegetation over a longer period of time. Figure 15 provides an illustration of the difference between these areas of analysis for a given time slice.

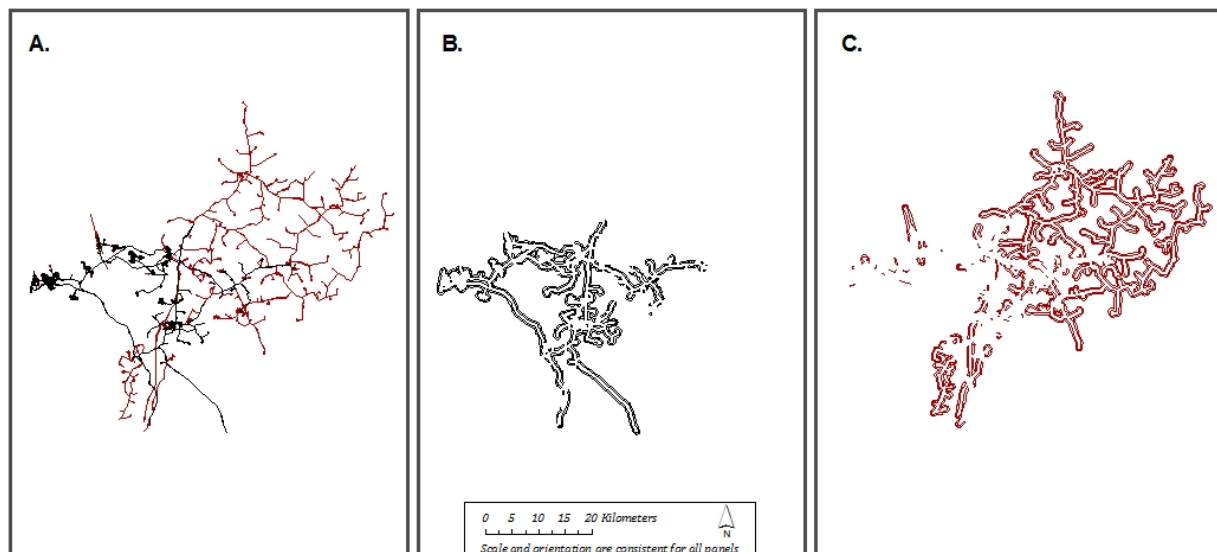


Figure 15. An illustration of the different extents employed in the calculation of change in mean NDVI values between two images. A) shows the extent of development in 1987 (black) and 1999 (red). B) shows the extent of previously developed areas. Delta mean NDVI values calculated for these areas capture the effects of vegetation recovery. C) shows the extent of newly developed areas. Delta mean NDVI values calculated for these areas reveal the effects of initial disturbance on vegetation communities adjacent to newly developed areas.

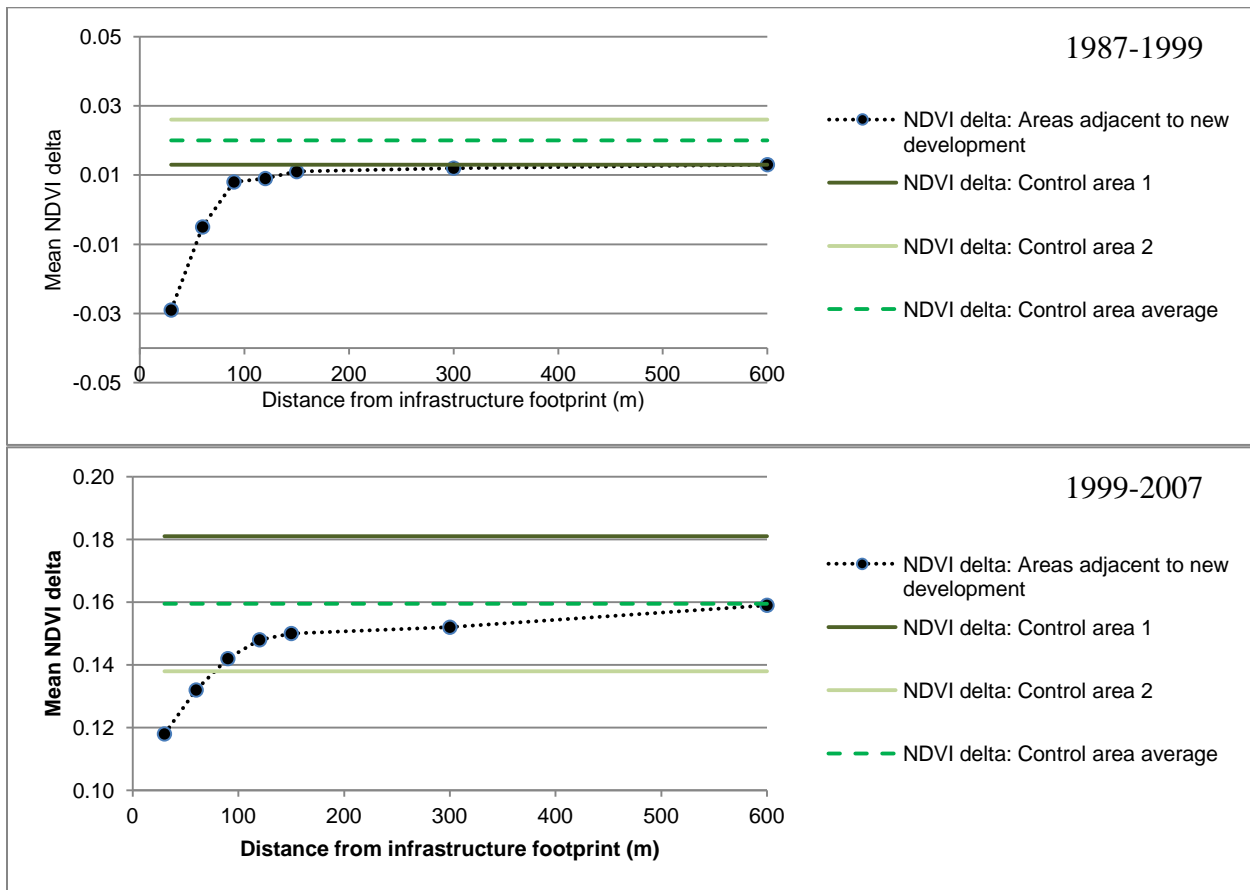


Figure 16. Changes in mean NDVI (delta NDVI) for areas adjacent to new development. Changes calculated for 1987 - 1999 (top) and 1999 - 2007 (bottom) show the effects of initial disturbance on NDVI values within 30–600 m of the development footprint between images. Scales on y-axis are different.

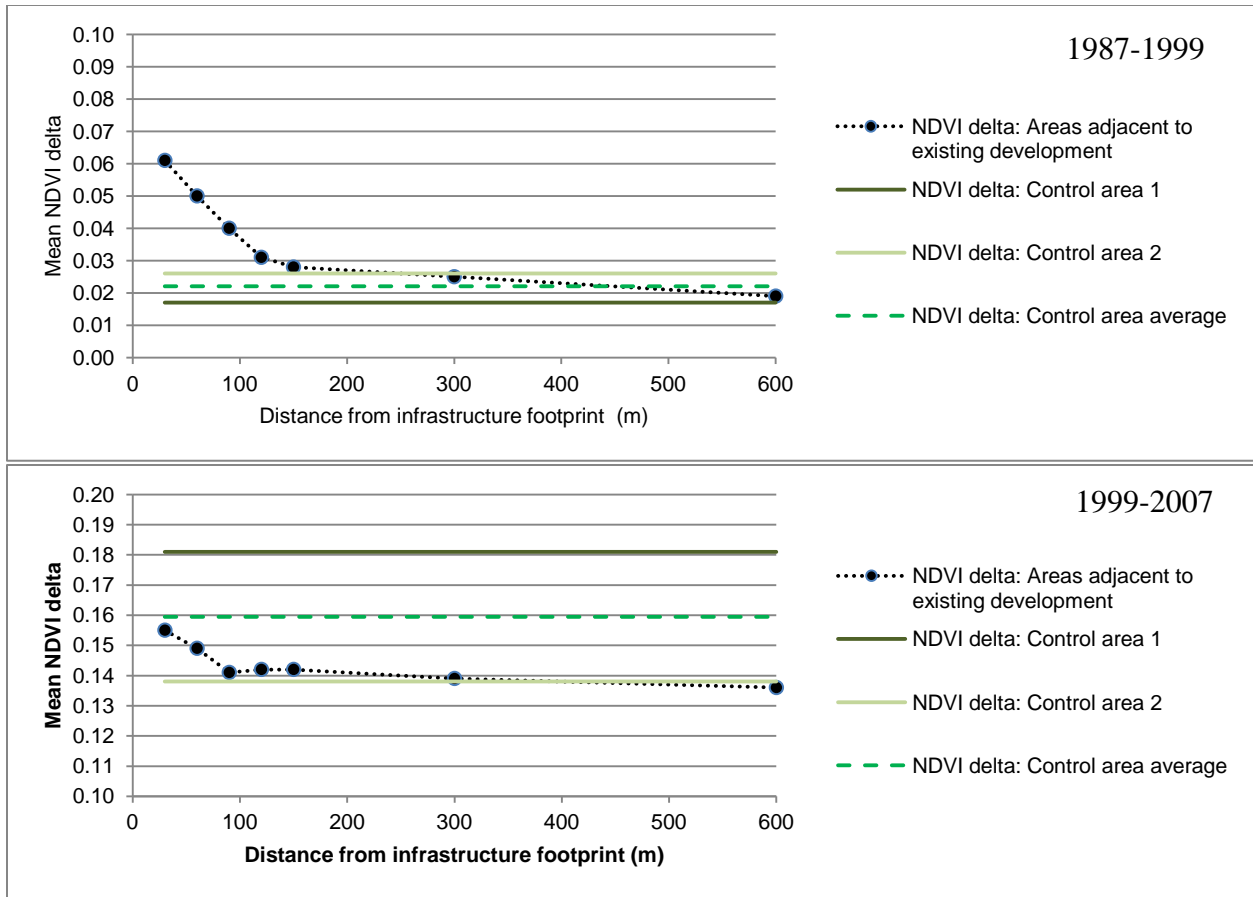


Figure 17. Changes in mean NDVI (delta NDVI) for areas adjacent to existing development. Changes calculated for 1987 - 1999 (top) and 1999- 2007 (bottom) show the effects of vegetation recovery on NDVI values for areas that have been developed prior to the calculated interval. Scales on y-axes are different.

In areas of new development, delta mean NDVI values are lower than those observed in control areas. This reduction gradually diminishes as distance from development increases, approaching the control area means (Figure 16). Conversely, in areas that were previously developed, delta mean NDVI values are larger than those observed in control areas. This positive difference similarly diminishes as distance from development increases, approaching the control area means (Figure 17).

This directional difference in delta mean NDVI values is consistent with the pattern of disturbance and recovery of vegetation communities (Pickett & White 1985). The impacts of initial disturbance on vegetation communities adjacent to new development results in a negative change in delta mean NDVI values as vegetated pixels are disturbed. These impacts can take many forms: complete eradication of vegetation as part of construction, diminished vegetation health resulting from increased dust or other impacts, or alterations to the previously existing surface hydrology that may change vegetation community composition were all observed by the author in the field near new construction. As the distance from development increases, these impacts are less severe, with both comparison time slices exhibiting stabilizing delta values at ~150 m.

Areas that have been previously developed show an increased delta NDVI response in comparison to control areas. As distance from development increases, the heightened delta NDVI values decrease, approaching the control area means at 90 m in the 1987-1999 interval. Delta mean NDVI values for the 1999-2007 interval approach the mean delta values calculated for control area 2 at ~150 m, although values are still decreasing at the lateral extent of the analysis (600 m). Causes of increased delta NDVI values in areas of previous development presumably indicate that these areas are becoming revegetated following initial disturbance. It is important to note that while delta NDVI values are higher than those observed in control areas, these values do not indicate a post-disturbance vegetation community that is more vigorous than undisturbed areas. Change values are elevated only due to the increased response manifested as previously unvegetated areas establish new vegetation communities. Because undisturbed areas have not experienced an initial disturbance impact, change values calculated for these areas are lower in comparison.

This analysis of changes in delta mean NDVI relative to development status over time reveals a strong pattern of impact on vegetation vigor in areas adjacent to development. In areas that have been previously developed, delta NDVI values show increased vegetation response as previously disturbed areas recolonize and adjust to alterations in geomorphology, use patterns, and surface hydrology. In areas that experience new development, delta NDVI values show an increased negative response when compared to control areas, reflecting the immediate impacts of infrastructure development upon previously undisturbed tundra vegetation. These changes appear most pronounced within 150 m of development, which is consistent with the extents of anthropogenic disturbance found by Vilchek and Bykova (1992) and Walker (1987). The cross-tabulation analysis described in the next section will further illustrate the nature of this change by identifying the directional changes of the individual pixel values that comprise the delta mean NDVI.

4.4 Cross tabulation of change in mean NDVI

Cross tabulations were calculated for both control areas and for the three distance intervals from the infrastructure as described in section 3.3.6. The cross tabulation outputs identify specific pixel changes between images that contribute to the changes in delta mean NDVI as described in the previous two sections. NDVI values for each pixel were reclassified according to the values in Table 3 in section 3.3.6. Figure 18 provides an illustration of the cross-tabulation analysis. Appendix B provides the complete cross-tabulation tables for each time interval.

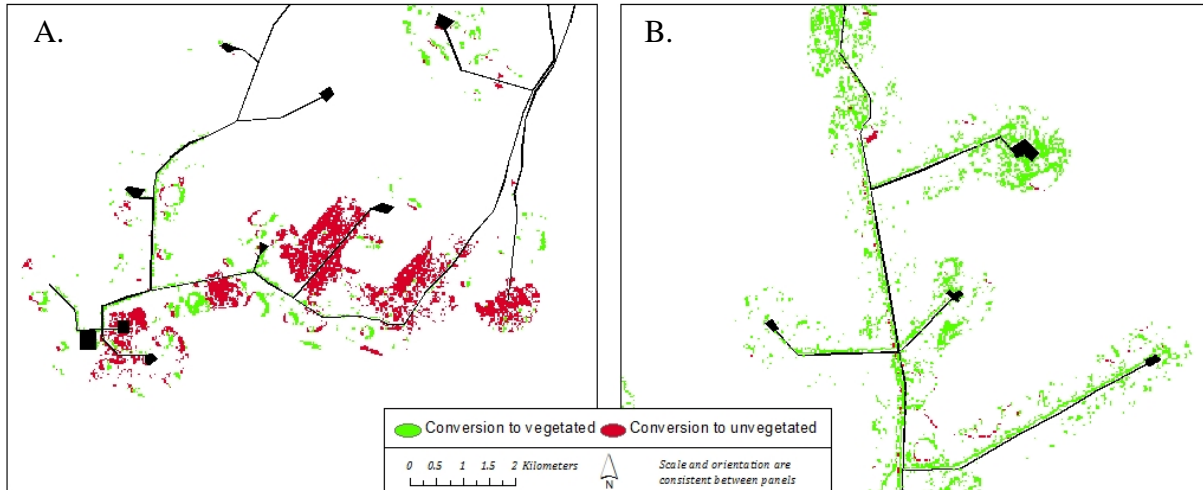


Figure 18. Example cross tabulation outputs showing conversion from vegetated to unvegetated pixels in an area of new development (A), and conversion from unvegetated to vegetated pixels in an area of existing development (B).

4.4.1 Cross tabulation of change from 1987 to 1999

The delta mean NDVI analysis performed for newly developed areas between 1987 and 1999 revealed depressed delta mean NDVI values within ~ 90 to 150 m of infrastructure (Figure 16). The cross-tabulation analysis for this observed change revealed that this decrease in greening is due to previously vegetated areas converting to barren or water classes. For newly developed areas between 1987 and 1999, 25% of pixels within the first 30 m buffer transitioned from a vegetated class to a barren or water category while 15% of pixels transitioned from a non-vegetated class to a vegetated class. For control areas through the same period, just 4% of pixels transitioned from a vegetated class to a barren or water class, while 15% of pixels transitioned from a non-vegetated class to a vegetated class (Table 5). As a function of relative area, tundra within the first 30 m of infrastructure converted to an unvegetated state at roughly five times the rate observed in control areas. These differences in change values dissipate as distance from the

infrastructure footprint increases, approaching values calculated for control areas in the outer buffers (Figure 19).

Conversely, the delta mean NDVI analysis performed on previously developed areas between 1987 and 1999 identified increased greening of areas within the first 90 m to 150 m of the infrastructure footprint when compared to changes in control areas (Figure 17). The cross-tabulation analysis revealed that this increased greening is due primarily to barren or water classes converting to vegetation. For previously developed areas between 1987 and 1999, just 3% of pixels within the first 30 m buffer transitioned from a vegetated class to a barren or water class, while 41% of pixels transitioned from a non-vegetated class to a vegetated class. For control areas during the same time period, approximately 4% of pixels transitioned from a vegetated class to a barren or water class, while 15% of pixels transitioned from a non-vegetated class to a vegetated class. The differences between observed rates of conversion from unvegetated to vegetated classes in this closest buffer is equal to approximately three times observed conversion rates in control areas. The pronounced difference between the changes observed in previously developed areas and control areas diminishes as distance from the infrastructure footprint increases, eventually reaching similar values at the 600 m extent of the analysis (Figure 19).

Table 5. Summary of conversion between vegetated and unvegetated classes in areas of new development between 1987 and 1999.

Distance	Vegetated to Unvegetated			Unvegetated to Vegetated		
	Area (km ²)	Area (%)	Departure from control (%)	Area (km ²)	Area (%)	Departure from control (%)
0-30m	8.32	24.8	20.8	4.91	14.6	-1.7
30-90m	9.8	14.5	10.5	10.89	16.1	-0.2
90-600m	33.14	7.4	3.4	79.92	17.7	1.4

Table 6. Summary of conversion between vegetated and unvegetated classes in areas of existing development between 1987 and 1999.

Distance	Vegetated to Unvegetated			Unvegetated to Vegetated		
	Area (km ²)	Area (%)	Departure from control (%)	Area (km ²)	Area (%)	Departure from control (%)
0-30 m	0.58	3	-1	8.14	42.1	25.8
30-90 m	2.28	6	2	12.94	34.2	17.9
90-600 m	17.4	6.5	2.5	65.95	24.6	8.3

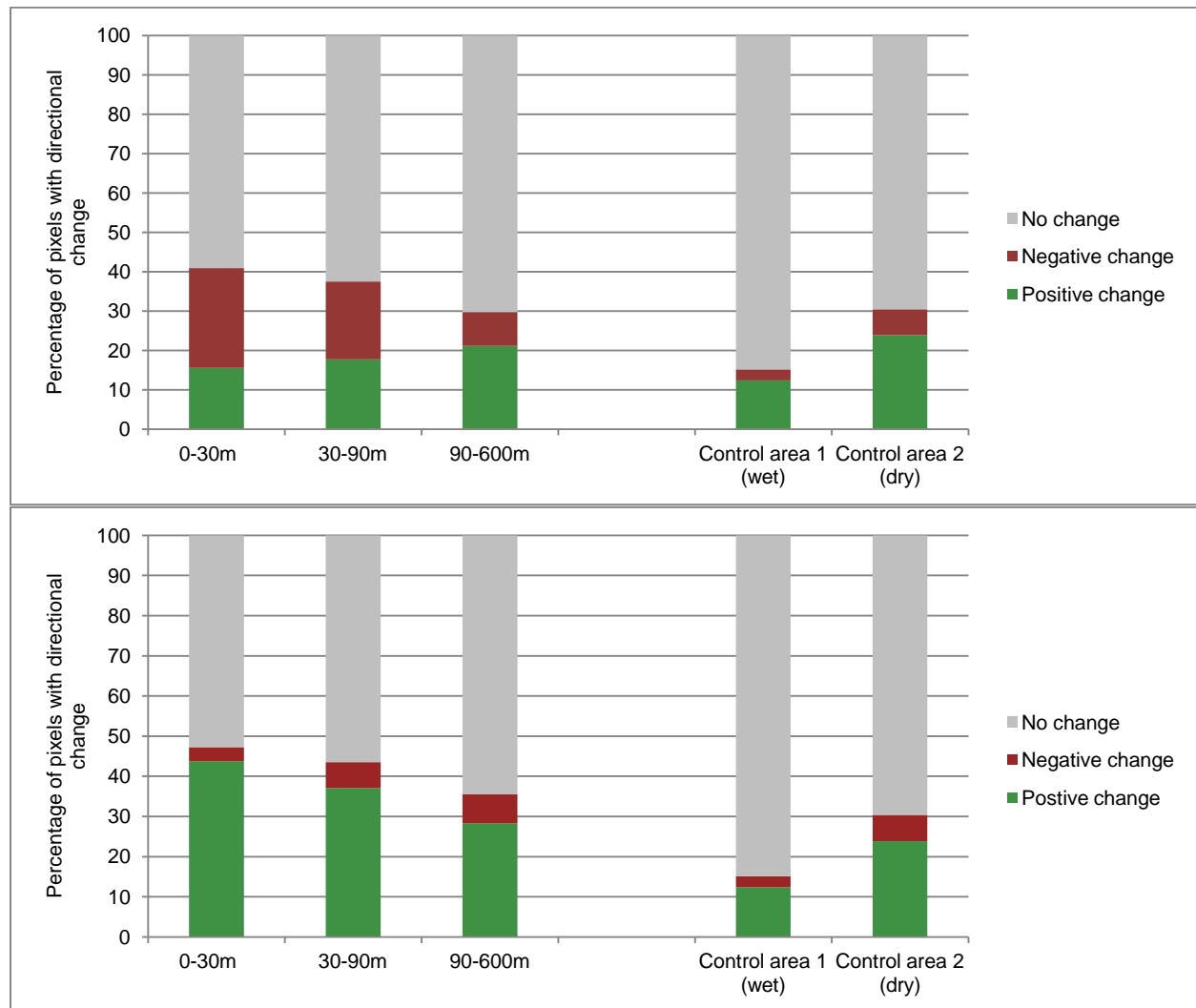


Figure 19. Summary of directional change in NDVI pixel values between 1987 and 1999. For newly developed areas (top), negative delta NDVI values are the result of initial disturbance where previously vegetated pixels transition to a non-vegetated state. For areas of existing development (bottom), positive delta NDVI values are the result of vegetation recovery where non-vegetated pixels become revegetated following initial disturbance.

4.4.2 *Cross tabulation of change from 1999 to 2007*

Cross tabulation for changes in delta mean NDVI values between 1999 and 2007 follow the pattern observed in the 1987-1999 time slice analysis (Figure 20). Negative changes between 1999 and 2007 are somewhat mitigated however, due to the fact that the 2007 scene has substantially higher overall NDVI values when compared to the 1987 and 1999 scenes. Mean NDVI values calculated for undisturbed control areas (as described in section 4.2) were stable between the 1987 and 1999 images (0.15 and 0.14, respectively), but then increased substantially to 0.30 in 2007. Because mean NDVI values between 1987 and 1999 were so similar, analyzed pixels revealed more pronounced directional change. In the 1999 to 2007 analysis, this directional change is still evident, but it appears primarily as relative increases or decreases in the percentage of pixels that undergo a positive change, as opposed to the more even distribution of positively and negatively changing pixels in the earlier time slice. The effects of observed differences in mean NDVI on this analysis is discussed in greater detail in section 4.4.3 below.

The effects of initial disturbance in the 1987 to 1999 interval were evidenced by a higher percentage of pixels that changed from vegetated to unvegetated NDVI values in the areas closest to development (Table 7). This diminished with distance, approaching control area values in the 90 – 600 m buffer (Figure 19). Similar patterns were found in the 1999 to 2007 interval, but the percentage pixels with values associated with barren land cover was much lower due to the overall higher mean NDVI values during this time period (Figure 20). Approximately 5% of pixels within the first 30 m showed a negative transition in the 1999 to 2007 analysis, compared to an average negative change of 0.5% within the control area. The percentage of pixels changing to barren or water decreased to approximately 2% within the 90 – 600 m buffer.

The pattern of negatively-shifting pixels was complemented by an increase in pixels that underwent a positive change as distance from new development increased. This suggests that in addition to converting vegetated areas to bare ground or water, new development had an additional impact on the vigor of areas that remain vegetated. Within the first 30 m, 53% of pixels show increased vigor, but this climbs to 69% within the 90-600 m buffer.

Observed changes within areas adjacent to existing development between 1999 and 2007 also followed the pattern established within the 1987 to 1999 interval (Table 8). Approximately 62% of pixels within the first 30 m of existing development show increased vegetative vigor, compared to an average of 52% within the control areas. Positive change values approach control area means within the 90-600 m interval, dropping to 53%.

Table 7. Summary of conversion between vegetated and unvegetated classes in areas of new development between 1999 and 2007.

Distance	Vegetated to Unvegetated			Unvegetated to Vegetated		
	Area (km ²)	Area (%)	Departure from control (%)	Area (km ²)	Area (%)	Departure from control (%)
0-30m	0.7	4.6	4.1	3.83	25.15	4.4
30-90m	0.15	2.72	2.2	6.82	21.31	0.6
90-600m	4.39	2	1.5	42.37	19.34	-1.4

Table 8. Summary of conversion between vegetated and unvegetated classes in areas of existing development between 1999 and 2007.

Distance	Vegetated to Unvegetated			Unvegetated to Vegetated		
	Area (km ²)	Area (%)	Departure from control (%)	Area (km ²)	Area (%)	Departure from control (%)
0-30m	0.5	1.1	0.5	21.6	44.6	23.9
30-90m	1.1	1.1	0.6	33.2	33.1	12.3
90-600m	9.3	1.3	0.8	150.6	21.5	0.8

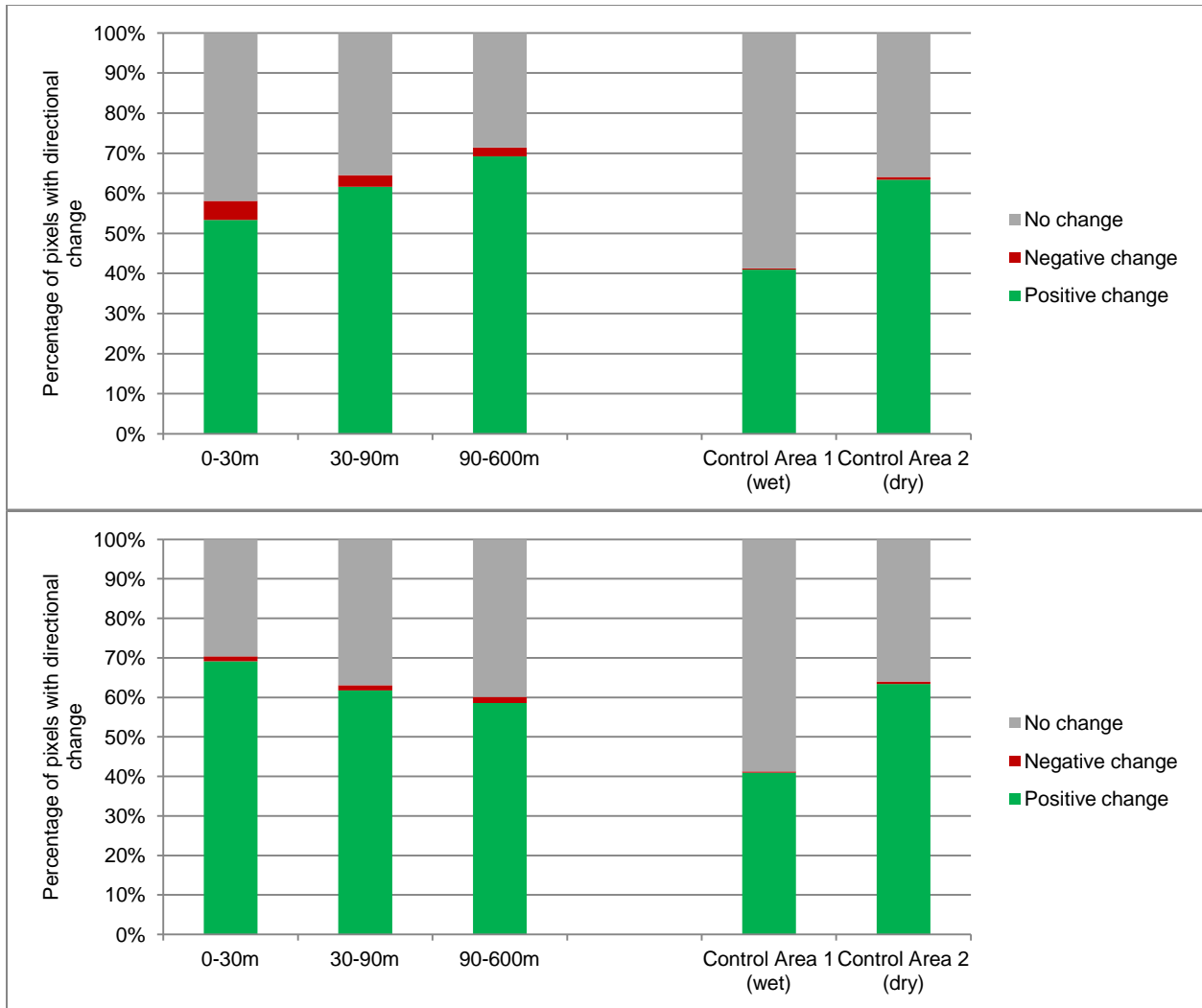


Figure 20. Summary of directional change in NDVI pixel values between 1999 and 2007. For newly developed areas (top), negative changes were greatest closest to development, showing an increased negative effect on vegetation as a result of initial disturbance. For areas of existing development (bottom), positive changes were greater in areas immediately adjacent to infrastructure, indicating a recovery response as previously disturbed areas revegetated.

4.4.3 Discussion

The cross-tabulation analysis above complements the mean delta NDVI analysis described in section 4.3 by showing which pixels contributed to observed changes. The results of the cross tabulation illustrate a pattern of vegetation disturbance and recovery areas adjacent to existing and new development within the Tazovsky peninsula. The majority of observed negative change in areas of new development is attributable to vegetated areas (classes 3 & 4)

transitioning to barren or water classes, as would be expected. The fact that the number of pixels that become unvegetated decreased as distance from disturbance increased, indicates that tundra vegetation becomes less affected by the impacts of development beyond the first 30 m, though it should be noted that negative change is still higher at the outer extents of the analysis than values observed in control areas.

Conversely, in areas of existing development, pixel values indicate increased vegetative vigor in the closest distance intervals. This suggests that previously disturbed areas are becoming revegetated and that additionally, observed effects of development such as soil disturbance and surface water ponding, have positive effects on recolonizing vegetation vigor. As discussed in section 2.2, this cannot necessarily be taken to mean that the community composition of new colonization is similar to the native vegetation which was initially disturbed. However, no data was available to the authors with which to evaluate species composition in the study area.

Cross tabulation outputs calculated for the 1999-2007 interval were complicated by higher overall NDVI values in the 2007 image. The increased NDVI values observed in 2007 can likely be attributed to the dates of the imagery. The 1987 image was collected in June, early in the growing season (some snow patches are still apparent), and the 1999 image was collected in September, toward the end of the growing season. The 2007 image however, was collected in July, at the peak of the growing season. Monthly NDVI composites from the Terra MODIS sensor illustrate monthly differences in NDVI over the course of each growing season within the study area (Figure 22)³. As this graph indicates, composite July values for 2007 are ~0.4 higher

³ It should be noted that monthly NDVI composite values are often higher than mean NDVI values calculated for individual scenes. This is due to the use of the Maximum Value Composite (MVC) method used to generate

than September values. Composite data are not available for 1999, but a graph of the 2000 composite data (the closest available year) is also included in Figure 21 to show that these phenological cycles are somewhat consistent between years.

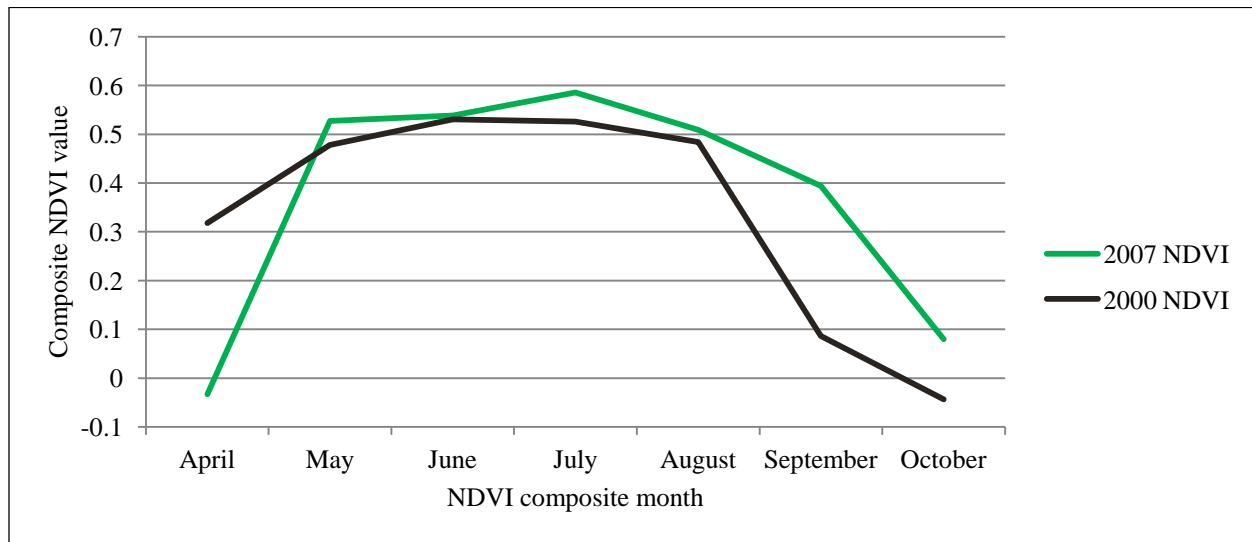


Figure 21. A graph showing monthly NDVI composite values calculated from 500 m resolution MODIS sensor on Terra for 2000 and 2007.

It would be expected then that the majority of observed pixel changes between 1999 and 2007 should be positive class transitions. The earlier interval analysis (1987-1999) showed that new development impacted the adjacent tundra by converting vegetated pixels to barren or water classes. These impacts are still evident in newly developed areas in the later analysis, but the more compelling evidence of development impacts is the reduced number of pixels that have undergone increased greening in the closest development buffers. The effects of the differences in seasonality between the imagery employed in this analysis are further discussed in Section 5.2.

monthly NDVI composites. The MVC seeks to minimize the effects of cloud cover by taking the highest measured NDVI values for each pixel within a given timeframe (Chen et al. 2003).

5 Conclusions and Future Research

5.1 Conclusions

The analyses summarized here establish quantitative evidence that infrastructure development has had measurable effects on both the landscape structure and vegetative composition of the Tazovsky peninsula. The fragmentation analysis quantified the degree to which the tundra has been fragmented by infrastructure development related to natural gas extraction and transport. The analysis of mean NDVI values indicates that vegetation vitality adjacent to developed areas is reduced compared to control areas of undeveloped tundra, and that this effect is most pronounced within 150 m of the infrastructure footprint (Figure 14). Analysis of the change in mean NDVI values over time shows that vegetation adjacent to newly developed areas exhibits a lowered NDVI response when compared to control areas, indicating that construction of new infrastructural elements has an immediate negative impact on adjacent vegetation (Figure 16). This analysis also revealed that vegetation adjacent to previously developed areas shows a positive NDVI response as vegetation communities reestablish in previously disturbed areas (Figure 17). The cross-tabulation analyses showed that the greening was attributable to the colonization of previously barren areas, while decreased NDVI change values indicated a conversion from vegetation to barren or water features (Figure 19 and Figure 20, Appendix B).

These conclusions are not wholly satisfying. That the landscape is becoming increasingly fragmented by development is indisputable. Vegetation response as measured through NDVI values, on the other hand, does not lend itself to concrete interpretations of changes in vegetation health and species composition. The negative response associated with new development suggests an ecologically destructive impact in the years following new construction, but the

subsequent increased greening seen in areas where infrastructure has existed for a longer period of time indicates that disturbed areas will recolonize. Identifying the post-disturbance composition of new vegetation communities is beyond the scope of this research, but existing research has shown that the composition of post-disturbance vegetation communities is often much different than those that existed prior to development (Forbes 1997, 1999; Khitun & Rebristraya 2002).

These results correspond well to previous work predicting spatial extents of the impacts related to infrastructure development on tundra landscapes and add to the literature by quantifying the impacts of the Yamburg field. The quantitative outputs of this research will not be precisely replicated in other areas of future development, but demonstrate that it is possible to quantify some of the impacts on surrounding tundra and to monitor the extents of disturbance during the various phases of new construction in northern Siberia and other regions. This case study demonstrates the strength of freely-available remotely sensed imagery to assess environmental impacts of anthropogenic development in environments where field-based assessment methods are not be practical or possible.

5.2 Analysis limitations and future research

As discussed above, the research presented in this thesis provided only a limited framework for evaluating the impacts of infrastructure development on tundra landscapes. Identifying the presence of differences in vegetation health in areas adjacent to development is important, but evaluating the species compositions and fine-scale changes that comprise those differences would help guide future disturbance mitigation.

The resolution of this analysis was limited by the available imagery employed. For the purposes of this research, the 30×30 m pixel resolution was sufficient to identify impacts in areas adjacent to development, but the results that could be conveyed by higher spatial and spectral resolution analyses would likely be more informative. Differences in mean NDVI and NDVI change values over time were consistently observed within the first 150 m from infrastructure – the use of higher spatial and spectral resolution imagery or field-based transects would facilitate detailed descriptions on the changes in vegetation, geomorphology, and surface hydrology that manifests these differences.

The temporal resolution of this analysis was similarly limited by available imagery collection dates. Again, although differences between imagery dates were identified in the current analysis, a finer temporal resolution would provide considerably more information on vegetation response patterns to new and existing development over time. With the patterns identified at this scale, endeavoring to perform a similar analysis on an annual or even seasonal basis would likely yield informative data to guide future development in the region. This research was initiated before the release of the Landsat imagery archives in 2009. With this additional body of remotely-sensed imagery available at no cost, future iteration of this research could employ additional dates and potentially yield more comprehensive results. It should be noted however that while many landscape-change assessments are moving to multiple scenes within each growing season, the prevalence of cloud cover in the Arctic will continue to be a factor that compromises the use of remotely-sensed imagery in analyses of Arctic regions.

The variability in NDVI values between imagery analyzed in this thesis is discussed in sections 3.3.2 and 4.4.2 as being at least partly attributable to seasonal differences between image collection dates. Mean NDVI values calculated for the 2007 imagery is roughly twice

those calculated for the 1987 and 1999. A byproduct of this difference is that analyses of change between 1999 and 2007 are likely skewed by the overall greening that occurs between these two scenes. Specifically, revegetation trends observed between 1999 and 2007 are likely overestimated, while initial disturbance effects are likely underestimated. Further analyses that employ this data would benefit from re-scaling calculated change values between years based on the observed change in overall mean NDVI. By accounting for the annual variability in mean NDVI, the remaining change values could more reliably be interpreted as the result of adjacent infrastructural development.

Private ownership of the study area, and the resulting limitations to data availability and field access limits the amount of ground-truthing or accuracy assessment that can be performed on the findings of this analysis. As mentioned in section 3.1.2, identification of the infrastructural footprint at each time slice was based in part on visual interpretation of the remotely-sensed imagery. The resulting digitization of these areas likely contains errors of omission as areas of questionable development status were not included in the final infrastructure layer. Additionally, buried and elevated pipelines were not able to be visually identified with confidence and were therefore not included. Thus, fragmentation as a result of pipelines is not included in this assessment which would also under-state the true fragmentation of the study area. This likely means that the total extent of explicit development and the effects that development has on the adjacent tundra, are underestimated in this analysis. Similarly, the cross-tabulation results rely on reclassified data that has been given ecological meaning. While the results of this analysis were compelling, the findings would benefit from field verification of the resulting classes (e.g. vegetated and unvegetated areas).

The fragmentation analysis performed for this analysis employed only the most basic metrics to illustrate the increasing fragmentation of undisturbed tundra patches in the study area. Fragmentation analyses can provide useful information on habitat impacts and use patterns by animal species when examined in the context of specific ecological criteria. Incorporating this additional species-level information when interpreting the fragmentation results presented in this analysis could yield meaningful results for further analyses on the biological impacts of resource infrastructure development in the study area, but the heterogeneity of tundra landscapes presents a consistent challenge to analyses that require high-resolution land-cover classifications.

The immediate impacts of infrastructure development in the study area, and the observed patterns of vegetation impacts in adjacent areas, constitute a compelling baseline assessment of landscape-level disturbance in the Tazovsky peninsula. Examining these preliminary findings at higher spatial, spectral, and temporal resolutions, and through the lens of specific ecological criteria, proffers the ability to make meaningful predictions on the impacts associated with future resource development in tundra landscapes. With the ability to predict future impacts, mitigation of those impacts on pristine tundra areas becomes a very real possibility.

6 References

- ACIA. (2004). *Impacts of a Warming Arctic: Arctic Climate Impact Assessment*. Cambridge: Cambridge University Press.
- Anderson, J. R., Hardy, E. E., & Witmer, R. E. (1976). *A Land Use and Land Cover Classification System for Use with Remote Sensor Data*. Washington, D.C.: United States Government Printing Office.
- Andren, H. (1994). Effects of Habitat Fragmentation on Birds and Mammals in Landscapes with Different Proportions of Suitable Habitat: A Review. *Oikos*, 355-366.
- Bykova, O. Y. (1995). Anthropogenic transformation of landscapes and analysis of ecological situation in Yamalo-Nenets Autonomous District. Moscow: Ph.D dissertation, Russian Academy of Sciences.
- Chander, G., Markham, B. L., & Helder, D. L. (2009). Summary of current radiometric calibration coefficients for Landsat MSS, TM, ETM+, . Remote Sensing of Environment, 893-903.
- Chen, P. Y., Fedosejevs, P., & Kiniry, J. R. (2003). Evaluating different NDVI composite techniques using NOAA-14 AVHRR data. *International Journal of Remote Sensing*, 3403-3412.
- Energy Information Association. (2010). *Summary of Russian Natural Gas Resources*. Washington, D.C.: U.S. Department of Energy.
- Energy Information Association. (1997). *Oil and Gas Resources of the West Siberian Basin, Russia*. Washington, D.C.: U.S. Department of Energy.
- Fahrig, L. (1997). Relative effects of habitat loss and fragmentation on population extinction. *Journal of Wildlife Management*, 603-610.
- Fleming, M. D. (1997, January). A statewide vegetation map of Alaska using phenological classification of AVHRR data. CAVM - North American Workshop . Anchorage, Alaska.
- Forbes, B. C. (1997). Tundra disturbance studies IV: Species establishment on anthropogenic primary surfaces, Yamal peninsula, northwest Siberia, Russia. *Polar Geography*, 79-100.
- Forbes, B. C. (1999). Land use and climate change on the Yamal Peninsula of north-west Siberia: some ecological and socio-economic implications. *Polar Research*, 367-373.
- Forbes, B. C., & Jeffries, R. L. (1999). Revegetation of disturbed arctic sites: constraints and applications. *Biological Conservation*, 15-24.
- French, H. (2003). The Development of Periglacial Geomorphology: 1 - up to 1965. *Permafrost and Periglacial Processes*, 29-60.

- Frey, K. E., & Smith, L. C. (1997). How well do we know northern land cover? Comparison of four global vegetation and wetland products with a new ground-truth database for West Siberia. *Global Biochemical Cycles*.
- Gazprom Dobycha Yamburg. (2007, July). Informational and Promotional Materials. Yamburg, Russia.
- Goetz, S. J., Bunn, A. G., Fisk, G. J., & Hough, R. (2005). Satellite-observed photosynthetic trends across boreal North America associated with climate and fire disturbance. *Proceedings of the National Academy of Sciences*. Washington, D.C.: National Academy of Sciences.
- Harrison, S., & Bruna, E. (1999). Habitat Fragmentation and Large-Scale Conservation: What do we know for sure? *Ecography*, 225-232.
- International Energy Agency. (2009). *Russia-EU Energy Dialogue: Report of Energy Infrastructure*. Retrieved 2007, from www.iea.org
- Khitun, O., & Rebristraya, O. (2002). Anthropogenic impacts on habitat structure and species richness in the West Siberian Arctic. *USDA Forest Service Proceedings* (pp. 85-95). Anchorage, AK: U.S. Department of Agriculture.
- Kryuchkov, V. V. (1993). Extreme Anthropogenic Loads and the Northern Ecosystem Condition. *Ecological Applications*, 622-630.
- Lachenbruch, A. H. (1970). Some estimates of the thermal effects of a heated pipeline in permafrost. Washington, D.C.: U.S. Geological Survey.
- Li, X., Lu, L., Cheng, G., & Xiao, H. (2001). Quantifying landscape structure of the Heihe River Basin, north-west China using FRAGSTATS. *Journal of Arid Environments*, 521-535.
- Lillesand, T. M., Kiefer, R. W., & Chipman, J. W. (2004). *Remote Sensing and Image Interpretation*. New York City, New York: John Wiley and Sons, Inc.
- Mahzitova, G., Karstkarei, N., Oberman, N., Romanovsky, V., & Kuhry, P. (2004). Permafrost and Infrastucture in the Usa Basin (Northeast European Russia): Possible Impacts of Global Warming. *Ambio*, 289-294.
- McGarigal, K., Cushman, S. A., Neel, M. C., & Ene, E. (2002). *FRAGSTATS: Spatial Pattern Analysis Program for Categorical Maps*. Amherst, Massachusetts, U.S.A.: Univeristy of Massachusetts.
- North, R. (1972). Soviet Northern Development: The case of NW Siberia. *Soviet Studies*, 171-199.
- O'Neill, R. V., Milne, B. T., Turner, M. G., & Gardner, R. H. (1988). Resource utilization sclaes and landscape pattern. *Landscape Ecology*, 63-69.
- Pickett, S., & White, P. (1985). *The Ecology of Natural Disturbance and Patch Dynamics*. San Diego, CA: Academic Press.

- Raynolds, M. K., Comiso, J. C., Walker, D. A., & Verblya, D. (2008). Relationship between satellite-derived land surface temperatures, arctic vegetation and NDVI. *Remote Sensing of Environment*, 1884-1894.
- Raynolds, M. K., Walker, D. A., & Maier, H. A. (2006). NDVI patterns and phytomass distribution in the circumpolar Arctic. *Remote Sensing of Environment*, 271-281.
- Schneider, M. F. (2001). Habitat Loss, fragmentation, and predator impact: spatial implications for prey conservation. *Journal of Applied Ecology*, 720-735.
- Shchelkunova, R. P. (n.d.). Geobotanical map of Yakutsk ASSR, scale 1:500000. Roszemproyekt, Saratov, USSR.
- Shiklomanov, N. I., & Nelson, F. E. (1999). Analytic representation of the active layer thickness field, Kuparuk River basin, Alaska. *Ecological Modelling*, 105-125.
- Southworth, J., Munroe, D., & Nagenda, H. (2004). Land cover change and landscape fragmentation - comparing the utility of of continuous and discrete analyses for a western Honduras region. *Agriculture, Ecosystems and Environment* , 185-205.
- Stow, D., Hope, A., Boynton, W., Phinn, S., Walker, D., & Auerbach, N. (1998). Satellite-derived vegetation index and cover type maps for estimating carbon dioxide flux for arctic tundra regions. *Geomorphology*, 313-327.
- Toutoubalina, O. V., & Rees, W. G. (1999). Remote sensing of industrial impact on Arctic vegetation around Noril'sk, norther Siberia: preliminary results. *International Journal of Remote Sensing*, 2979-2990.
- U.S.G.S. (2009, October 6). Land Processes Distributed Active Archive Center. Retrieved May 2012, from MRT Web: https://lpdaac.usgs.gov/get_data/mrtweb
- Ulmishek, G. F. (2003). *Petroleum Geology and Resources of the West Siberian Basin, Russia*. Reston, VA: U.S. Geological Survey.
- University of Maryland. (2012). Global Land Cover Facility Earth Science Data Interface. Retrieved March 2007, from www.landcover.org
- Vilchek, G. E., & Bykova, O. Y. (1992). The Origin of Regional Ecological Problems with the Northern Tyumen Oblast, Russia. *Arctic and Alpine Research*, 99-107.
- Walker, D. A., Bay, C., Daniels, F., Einarrsson, E., Elvebakk, A., Johansen, B. E., et al. (1995). Toward a new arctic vegetation map: A review of existing maps. *Journal of Vegetation Science*, 427-436.
- Walker, D. A., & Everett, K. R. (1987). Road dust and its environmental impact on Alaskan taiga and tundra. *Arctic and Alpine Research*, 479-489.
- Webber, P. J., & Ives, J. D. (1978). Damage and Recovery of Tundra Vegetation. *Environmental Conservation*, 171-182.

Weier, J., & Herring, D. (n.d.). Measuring Vegetation (NDVI and EVI). Retrieved July 2011, from NASA Earth Observatories:
<http://earthobservatory.nasa.gov/Features/MeasuringVegetation/>

Weller, C., Thomson, J., Morton, P., & Aplet, G. (2002). *Fragmenting Our Lands: The ecological footprint from oil and gas development. A spatial analysis of a wyoming gas field.* The Wilderness Society.

Zhou, L., Tucker, C. J., Kaufmann, R. K., Slayback, D., Shabanov, N. V., & Myeni, R. B. (2001). Variations in northern vegetation activity inferred from satellite data of vegetation index during 1981 to 1999. *Journal of Geophysical Research*, 20069-20083.

Appendices

Appendix A. A list of vegetation species found within the western Siberian tundra.

Latin name	Common name
<i>Alnus fruticosa</i>	Siberian alder
<i>Andromeda polifolia</i>	bog rosemary
<i>Arctous alpina</i>	alpine bearberry
<i>Artemisia vulgaris</i>	mugwort (or wormwood)
<i>Betula nana</i>	dwarf birch
<i>Betula nana exilis</i>	dense cover birch
<i>Betula pendula</i>	silver birch
<i>Carex spp.</i>	sedge species
<i>Cetratia islandica</i>	island cetraria lichen
<i>Chamaenaerium angustifoliaum</i>	fireweed
<i>Comarum palustre</i>	purple marshlocks
<i>Deschampsia caespitosa</i>	tufted hairgrass
<i>Empetrum nigrum</i>	crowberry
<i>Equisetum pratense</i>	shady horse grass or horsetail
<i>Erioporum vaginatum</i>	tussock cottongrass
<i>Juniperus sibirica</i>	Siberian juniper
<i>Larix sibirica</i>	Siberian larch
<i>Ledum palustre</i>	marsh Labrador tea
<i>Papaver polare</i>	Svalbard poppy
<i>Picea abis</i>	Norway spruce
<i>Poa spp.</i>	grass species
<i>Polemonium acutiflorum</i>	tall Jacob's-ladder
<i>Rubus chamaemorus</i>	cloudberry
<i>Salix lanata</i>	woolly willow
<i>Salix polaris</i>	polar willow
<i>Salix pulchra</i>	tealeaf willow
<i>Sphagnum balticum</i>	Baltic sphagnum
<i>Tripleurospermum hukere</i>	wild chamomile
<i>Vaccinium uliginosum</i>	bog blueberry
<i>Vaccinium vitis</i>	lingonberry

Appendix B. Cross tabulation output tables. Categories are as follows: 1 – water; 2 - bare ground, snow, cloud, etc.; 3, 4, and 5 are vegetation with increasingly high vitality. Table on left is pixels, while right units are percentages.

Table 9. Summary of cross tabulation results calculated for newly developed areas between 1987 and 1999.

New development 1987 - 1999 (0-30m)						New development 1987 - 1999 (30-90m)						New development 1987 - 1999 (90-600m)							
1987 class						1987 class						1987 class							
1999 class						1999 class						1999 class							
	1	2	3	4			1	2	3	4			1	2	3	4		Control 1	Control 2
1	178	163	68	0	409	1	0.48	0.44	0.18	0.00	1.10	Positive	15.56	12.39	23.84				
2	307	9431	9152	22	18912	2	0.82	25.26	24.51	0.06	50.65	Negative	25.36	2.73	6.57				
3	122	5318	12447	63	17950	3	0.33	14.24	33.34	0.17	48.08	No change	59.08	84.88	69.59				
4	0	15	49	2	66	4	0.00	0.04	0.13	0.01	0.18								
	607	14927	21716	87	37337		1.63	39.98	58.16	0.23	100.00								
1	880	3778	127	0	4785	1	1.17	5.02	0.17	0.00	6.35	Positive	17.74	12.39	23.84				
2	1104	14783	10726	33	26646	2	1.47	19.63	14.24	0.04	35.38	Negative	19.73	2.73	6.57				
3	428	11611	31422	196	43657	3	0.57	15.42	41.72	0.26	57.97	No change	62.53	84.88	69.59				
4	5	54	161	4	224	4	0.01	0.07	0.21	0.01	0.30								
	2417	30226	42436	233	75312		3.21	40.13	56.35	0.31	100.00								
1	26242	4220	1018	4	31484	1	5.25	0.84	0.20	0.00	6.30	Positive	21.11	12.39	23.84				
2	15602	82142	35718	85	133547	2	3.12	16.43	7.15	0.02	26.72	Negative	8.59	2.73	6.57				
3	4790	83193	242942	1890	332815	3	0.96	16.64	48.60	0.38	66.58	No change	70.30	84.88	69.59				
4	87	732	1125	73	2017	4	0.02	0.15	0.23	0.01	0.40								
	46721	170287	280803	2052	499863		9.35	34.07	56.18	0.41	100.00								

Table 12. Summary of cross tabulation results calculated for areas of existing development between 1999 and 2007.

Existing development 1999 - 2007 (0-30m)							Existing development 1999 - 2007 (30-90m)							Existing development 1999 - 2007 (90-600m)													
1999 class							1999 class							1999 class													
	1	2	3	4	5			1	2	3	4	5			1	2	3	4	5			Control 1	Control 2				
2007 class	1	84	45	2	0	0	131	2007 class	1	0.16%	0.08%	0.00%	0.00%	0.00%	0.24%	Positive	69.17%	40.97%	63.42%	Negative	1.19%	0.29%	0.63%	No change	29.64%	58.73%	35.95%
	2	373	451	565	1	0	1390		2	0.69%	0.84%	1.05%	0.00%	0.00%	2.58%		1.19%	0.29%	0.63%								
	3	147	19645	15348	29	0	35169		3	0.27%	36.53%	28.54%	0.05%	0.00%	65.40%		29.64%	58.73%	35.95%								
	4	11	4178	12648	55	0	16892		4	0.02%	7.77%	23.52%	0.10%	0.00%	31.41%												
	5	0	22	150	22	0	194		5	0.00%	0.04%	0.28%	0.04%	0.00%	0.36%												
		615	24341	28713	107	0	53776			1.14%	45.22%	53.11%	0.16%	0.00%	100.00%												
2007 class	1	435	111	8	0	0	554	2007 class	1	0.39%	0.10%	0.01%	0.00%	0.00%	0.50%	Positive	61.79%	40.97%	63.42%	Negative	1.29%	0.29%	0.63%	No change	36.92%	58.73%	35.95%
	2	1189	6690	1258	1	0	9138		2	1.07%	6.00%	1.13%	0.00%	0.00%	8.20%		1.29%	0.29%	0.63%								
	3	412	31417	33775	63	0	65667		3	0.37%	28.20%	30.31%	0.06%	0.00%	58.94%		36.92%	58.73%	35.95%								
	4	34	4949	30418	234	0	35635		4	0.03%	4.44%	27.30%	0.21%	0.00%	31.98%												
	5	2	19	353	48	0	422		5	0.00%	0.02%	0.32%	0.04%	0.00%	0.38%												
		2072	43186	65812	346	0	111416			1.86%	38.74%	58.75%	0.27%	0.00%	100.00%												
2007 class	1	15895	1643	68	0	0	17606	2007 class	1	2.04%	0.21%	0.01%	0.00%	0.00%	2.26%	Positive	58.56%	40.97%	63.42%	Negative	1.58%	0.29%	0.63%	No change	39.85%	58.73%	35.95%
	2	29961	43696	10264	45	0	83966		2	3.85%	5.61%	1.32%	0.01%	0.00%	10.78%		1.58%	0.29%	0.63%								
	3	4813	140340	248981	292	0	394426		3	0.62%	18.03%	31.98%	0.04%	0.00%	50.66%		39.85%	58.73%	35.95%								
	4	510	21357	252823	1719	0	276409		4	0.07%	2.74%	32.47%	0.22%	0.00%	35.50%												
	5	13	300	5057	779	0	6149		5	0.00%	0.04%	0.65%	0.10%	0.00%	0.79%												
		51192	207336	517193	2835	0	778556			6.57%	26.59%	65.78%	0.26%	0.00%	100.00%												

